

UNIVERSITY OF GHANA

**GEOLOGY AND GEOCHEMISTRY OF PIT ROCKS FROM THE OBUEM
CONCESSION IN THE KONIYAW AREA - KUMASI**



**THIS THESIS IS SUBMITTED TO THE UNIVERSITY OF GHANA,
LEGON IN PARTIAL FULFILMENT OF THE REQUIREMENT FOR THE
AWARD OF M. PHIL GEOLOGY DEGREE**

JULY, 2014

DECLARATION

I hereby declare that, except for references to other people’s work which have been duly cited, this work is the result of the authors own studies conducted on the area that was mapped under supervision. This thesis has neither, in whole nor in part been submitted for a degree either in this university or elsewhere.

AMOAKO ALFRED PREMPEH

.....

(ID. 10220899)

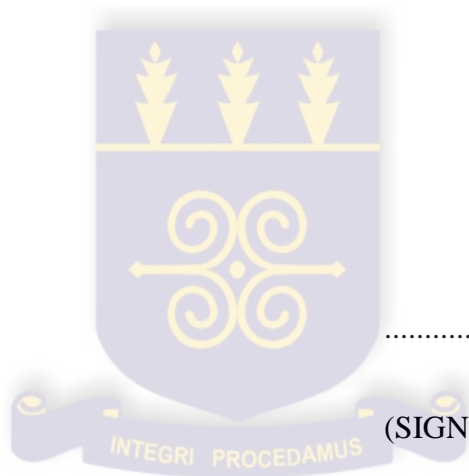
(SIGNATURE)

PROF. JOHNSON MANU

.....

(SUPERVISOR)

(SIGNATURE)



PROF. F. K. NYAME

.....

(SUPERVISOR)

(SIGNATURE)

DEDICATION

This report is first and foremost dedicated to God and then to my parents Mr. and Mrs. Amoako, my elder brothers and sisters whose efforts enabled me to go through my education and to all those whose assistance made this project possible.



ABSTRACT

Geological mapping and geochemical analysis of rock samples were made on pit rocks from Obuem Mining Concession found within the Birimian of Ashanti Belt of Ghana, in order to determine the nature of gold mineralisation. The study area consists of metavolcanics and metasediments with few intrusions of granitoids.

Metasediments such as phyllites and schists as well as metavolcanics of andesitic and basaltic origin were sampled and analyzed for their major and trace element contents using ICP-MS and XRF methods in order to constrain their provenance and source area weathering. The analyses of the metavolcanics indicate a tholeiitic nature.

The rate of alteration is fairly intense as indicated by the high loss of ignition values. Most of the primary minerals such as hornblende, biotite and plagioclase have been altered to sericite, epidote, chlorite and groundmass. These geochemical characteristics depict a mafic source for the phyllites dominantly consisted of.

The stretched, contorted grain crystals and the presence of quartz veins in the rocks affirm the dynamic nature of the metamorphism as they indicate that the area has experienced some level of tectonic activity and fairly significant amount of metamorphism. The quartz grains show extreme deformational effects as deformation crenulation. Average Cr and Ni abundances and Cr/Ni ratios of average phyllites of the Birimian metasediments indicate that the source consisted of basaltic material.

Geochemical data and tectonic discrimination diagram for the Birimian metasediments and metavolcanics suggest that few of the metasediments were deposited within a passive margin while majority of them in the passive continental margin.

ACKNOWLEDGEMENT

I am indebted to a large number of individuals and communities for assistance in bringing this report to completion. I would like to express my appreciation and gratitude to my supervisors Prof. Johnson Manu, and Prof. F. K. Nyame their mentoring and wonderful directions as well as their technical advice.

My next thanks go to all other lecturers in the department for their help in diverse ways (lectureship, field trips, personal relationships, etc). I am also grateful to the lab technicians and technical staff of the department for their contribution towards the preparation of thin sections.

I wish to thank Nana Apraku and his employees, as well as Mr. Biamah, all of Koniyaw - Bekwai for their hospitality during my field work. My Family also deserves great commendation for their encouragement throughout the study.

Then finally, I sincerely thank my course mates George Afrifa, Belinda S. Berdie, Dumolga Michael and junior friends of the MPhil Part 1 for their co-operation and help.

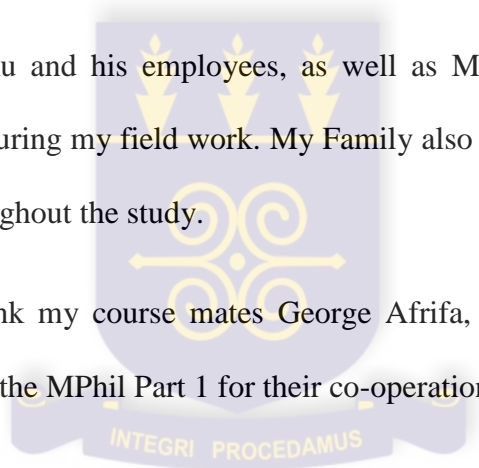
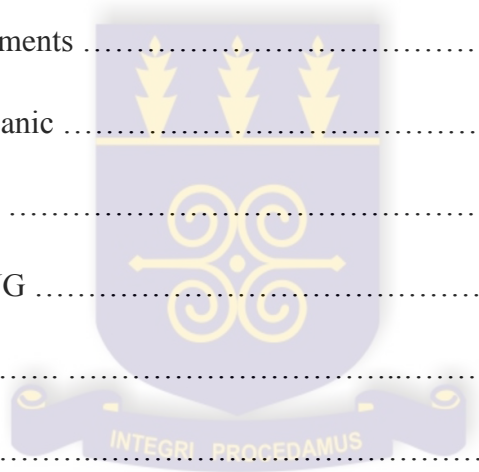


TABLE OF CONTENTS

DECLARATION	ii
DEDICATION.....	iii
ABSTRACT	iv
ACKNOWLEDGMENT	v
TABLE OF CONTENT	vi
LIST OF FIGURES	vii
CHAPTER ONE	1
INTRODUCTION	1
1.1 BACKGROUND	1
1.2 PROBLEM STATEMENT	2
1.3 RESEARCH OBJECTIVES	3
1.4 JUSTIFICATION	3
1.5 LOCATION AND PHYSIOGRAPHY	4
1.6 HISTORY	7
CHAPTERTWO	9
LITERATURE REVIEW	9
2.1 GLOBAL GEOLOGY	9
2.2 BIRIMIAN GEOLOGY (REGIONAL GEOLOGY)	11
2.3 LOCAL GEOLOGY	13
CHAPTER THREE	15
METHODOLOGY	15
3.1 INTRODUCTION	15
3.1.1 PRE-FIELD WORK	15
3.1.2 FIELD WORK	15

3.1.3 POST-FIELD WORK	18
3.3.1 Petrography	18
3.3.2 Preparation of thin sections	19
3.3.3 Geochemical analysis	20
CHAPTER FOUR	21
RESULTS	21
4.1 PETROGRAPHY	21
4.1.1 Granitoids	21
4.1.2 Metasediments	25
4.1.3 Metavolcanic	37
4.1.4 Quartzite	40
4.2 STRUCTURAL MAPPING	44
4.2.1 Joints	44
4.2.2 Folding	47
4.2.3 Lineation	50
4.2.4. Foliations	53
4.3 GEOCHEMISTRY	55
4.3.1. Composition of rock groupings	55
4.3.2. Classification of Metavolcanic rocks	58
4.3.3. Geochemistry of Metasediments	63
4.3.4. Classification of Granitoids	66



CHAPTER FIVE	69
DISCUSSION	69
5.1 MAGMA SOURCE AND TECTONIC SETTINGS	69
5.1.1. Tectonic settings	70
5.2 TECTONIC EVOLUTION AND DEFORMATION	71
5.3 MINERALISATION	71
5.4 METAMORPHISM AND ALTERATION	73
CHAPTER SIX	76
CONCLUSION AND RECOMMENDATION	76
6.1 CONCLUSION	76
6.2 RECOMMENDATION	79
REFERENCES	80

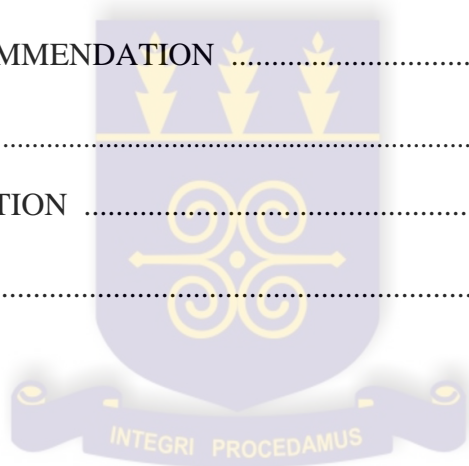


Figure 4.8	Photomicrograph of a Greywacke both in Crossed nicols and plane polarized light.....	34
Figure 4.9	Photograph of crystalline and veined metavolcanic rock at Obuem	37
Figure 4.10	Photomicrograph of a Chlorite-schist Crossed nicols and plane polarized light.	39
Figure 4.11	Photograph of well indurated quartzite at South of Obuem.	40
Figure 4.12	Photomicrograph of a Quartzite both in Crossed nicols.....	43
Figure 4.13	Photograph of quartzites that are thickly foliated and highly jointed widely jointed schist outcropping half way between Kokotro and Obuem.....	42.
Figure 4.14	Stereographic projection of (a) Rose diagram showing a general NW-SE strike of joints (b) Plot to poles of joints within the lithologies	43
Figure 4.15	Photograph showing an initial asymmetric folding S0 axis and fold outcropping at East of Obuem	44
Figure 4.16	Photograph showing (a) truncated fold axis and anticlinal asymmetric fold outcropping at East of Obuem	45
Figure 4.17	Stereographic projections of (a) plot of centroid of folds in rocks showing a north western – south eastern strike, and (b) rose diagram of folds	46
Figure 4.18	Photograph of a concordant Quartz vein leading from entrance into a mining pit. They are highly recrystallized.....	47
Figure 4.19	Photograph showing concordant and discordant Quartz veins in schist rock. Good cross cutting relationship.....	48

Figure 4.20	Stereographic projections of (a) plot of centroid of Quartz veins in rocks showing a west – north western strike, and (b) rose diagram of Quartz veins	49
Figure 4.21	Photograph of foliations observed in Metavolcanic	50
Figure 4.22	Photograph of crenulations observed in Greywacke	51
Figure 4.23	Photograph of thickly foliated Graphitic Phyllites	52
Figure 4.24	TAS Alkalis-Silica Classification of Obuem Mine metavolcanics on a $\text{Na}_2\text{O}+\text{K}_2\text{O}$ – SiO_2 diagram (after Middlemost 1975).	59
Figure 4.25	TAS Alkalis-Silica Classification of Obuem Mine metavolcanics on a $\text{Na}_2\text{O}+\text{K}_2\text{O}$ – SiO_2 diagram after LeBas et al., 1986	59
Figure 4.26a	AFM Triangular Plot showing boundary fields from the Obuem samples. (After Sun & McDonald (1989))	64
Figure 4.26b	The $\text{MnO}-\text{TiO}_2-\text{P}_2\text{O}_5$ discrimination diagram for basalts and basaltic andesites (after Mullen, 1983).	
Figure 4.27	Spider plots for the REE normalized against the Chondrite after Sun & McDonald (1989).....	64
Figure 4.28	Variations of Oxides versus SiO_2 samples from Obuem concession.....	64
Figure 4.29	Primordial mantle of metavolcanics	65
Figure 4.30	Spider plots for the REE normalized against the Chondrite after Sun & McDonald (1989).....	65

Figure 4.31	The chemical classification of plutonic rocks using their molecular normative compositional diagram. (after Streckeisen and Le Maitre 1979)	66
Figure 4.32	The chemical classification and nomenclature of plutonic rocks using the total alkalis versus silica (TAS) diagram. (after Cox et al, 1979)	67
Figure 4.33	Primordial mantle of granitoids.	67
Figure 4.34	Hf-Rb/30-Ta \times 3 discriminant diagram of arc maturity for volcanic granitoids (after Harris et al, 1986)	68
Figure 5.1	Plot showing the tectonic settings of the metasediments	69
Figure 5.2a	Primordial mantle of granitoids	70
Figure 5.2b	Hf-Rb/30-Ta \times 3 discriminant diagram of arc maturity for volcanic granitoids (after Harris et al, 1986)	70

LIST OF TABLES

Table 1	Representative compositions of major minerals from the Granitoid	23
Table 2	Representative compositions of major minerals from the metasediment.....	27
Table 3	Representative compositions of major minerals from the graywacke.....	35
Table 4	Representative compositions of major minerals from the metavolcanics.....	39
Table 5	Representative compositions of major minerals from the quartzite	42
Table 6:	Major elements of rock samples from the Obuem concession Ash Reg., Ghana.....	56
Table 7:	REEs of rock samples from the Obuem concession Ash Reg., Ghana.....	57
Table 8.	Trace Element of rock samples from the Obuem concession Ash. Reg., Ghana.....	63

Table 9: Major elements of Mafic rock samples from the Obuem concession Ash Reg., Ghana..... 63

Table 10: REE elements of Mafic rock samples from the Obuem concession Ash Reg., Ghana.....64

Table 11: Major elements of Metasediments from the Obuem concession in the Ash Reg., Ghana.....64

Table 12: REE of Metasediments from the Obuem concession in the Ash Reg., Ghana68

LIST OF ABBREVIATIONS

Ash. Reg	Ashanti Region
Bt	Biotite
Cal	Calcite
Chl	Chlorite
Grndms	Groundmass
Hbl	Hornblende
Mcl	Microcline
Py	Pyrite
Plg	Plagioclase
Qtz	Quartz
Grph	Graphite
ICPMS	Inductively Coupled Plasma-Mass Spectroscopy
PoQtz	Polycrystalline Quartz

LREE	Light Rare Earth Element
REE	Rare Earth Element
XRF	X-Ray Florescence

CHAPTER ONE

1.0 INTRODUCTION

1.1 BACKGROUND

Mineral deposit classification involves characterization and grouping of mineral deposits according to the attributes or features they exhibit (Seidu, 2007). Classification of mineral deposit occurrences is essential to mineral prospectivity mapping, because only one type of mineral deposit occurrences should be used in the analysis. The traditional way of mineral deposit classification is based largely on geologic characteristic of mineral deposits such as their ore mineralization, host rock lithology, wall rock alteration, timing and depth of ore formation, as well as geologic settings.

The Obuem concession gold deposit is similar in many ways to the lode deposits of the Ashanti belt that hosts the Obuasi gold mine. The structurally controlled ore body is a steep north to north-east trending shear corridor that is predominantly hosted by a metasedimentary package of metasediment and lesser volcanoclastics along with its subordinate granitoid intrusions. Mode of exploiting minerals in Obuem assert to the fact that gold mineralisation in the Birimian of Ghana occurs at the contact of the volcanic and sedimentary rocks and also in the graphitic shear zones of mafic volcanic rocks (Kesse, 1985; Perrouy, 2012). Gold mineralization is associated with quartz veins with about 3% arsenopyrite in the wall rock, which occurs largely along the edges or along cracks within sulphides.

The analysis of the structure and alteration relations of the study area would be deduced from the geochemistry and measured geological field attitudes of the igneous rocks to help determine the geotectonic environment under which the intrusive gold mineralization occurs on the field.

1.2 PROBLEM STATEMENT

Geological maps have been produced covering most parts of Ghana. Even in present times a more advanced geological map has been produced by a collaborative work of some professionals from the Ghana Geological Survey and Federal Republic of Germany. Nonetheless, these maps give a broad and general picture of the geology within a particular terrane. The geology of the Ashanti belt as produced for instance is as a result of intensive work done at the Obuasi mine.

The question, however, is whether this broad geological picture is really the same for the various other prospects that find themselves on this belt. There is therefore an urgent need to overcome the limited understanding of the local geology as well as parameters that determine the occurrence, availability and quality of this valuable resource.

Veining of rocks and alteration in mineralised rocks have been used by ‘learned’ local miners as path-finders or mineral associations in the means of discovering gold within this concession of this study area. This thesis would study the in-situ/local geology and correlate them to the bigger picture of the geology of the Ashanti belt. This study presents an integrated interpretation based on new field data, and previous structural studies and maps (Perrouy et al., 2012) that provides mineralization ideas to the Obuem concession of the Ashanti greenstone belt. A petrographic and geological analysis of the samples as well studies of the tectonic environment may help develop a genetic model for further exploration. The study would include briefly reviewing available data and embarking on field studies to know in detail the geology and structures of outcrops that would help in determining the nature of gold mineralization in this terrane.

It is hoped that the study would also contribute to the impending confirmation of alteration patterns to the interpretation of “Birimian” tectonic settings and estimations of the gold potential of the “Achaean volcano-sedimentary terranes”.

1.3 RESEARCH OBJECTIVES

The project is designed to achieve the following three objectives and will focus mainly on them:

1. Carrying out lithological mapping on the study area as well as picking of representative and oriented samples that characterize the lithologies observed.
2. The study of mineralogical composition, textures, structural features and any alteration features that would possibly help in obtaining the nature of gold mineralization of the concession.
3. Geochemically classifying rocks and studying alteration history to find out their genesis and relationships that exist between the host rock and the ore deposition.

All information derived would help to discern the geological history of the area and relate the study area to other gold belts in Ghana.

1.4 JUSTIFICATION

A prior knowledge of the geochemical characteristics of a not-well known and studied mineral deposit occurrences (as of this study area) is very indispensable in predicting a model for exploration targets. This research would study the surface and sub-surface materials in the study areas and provide more understanding to the local geology in geometric and spatial terms. This

will then add to the knowledge of Prospectors and Geologists as they compare or link rocks relationships to the major Ashanti gold belt of Ghana.

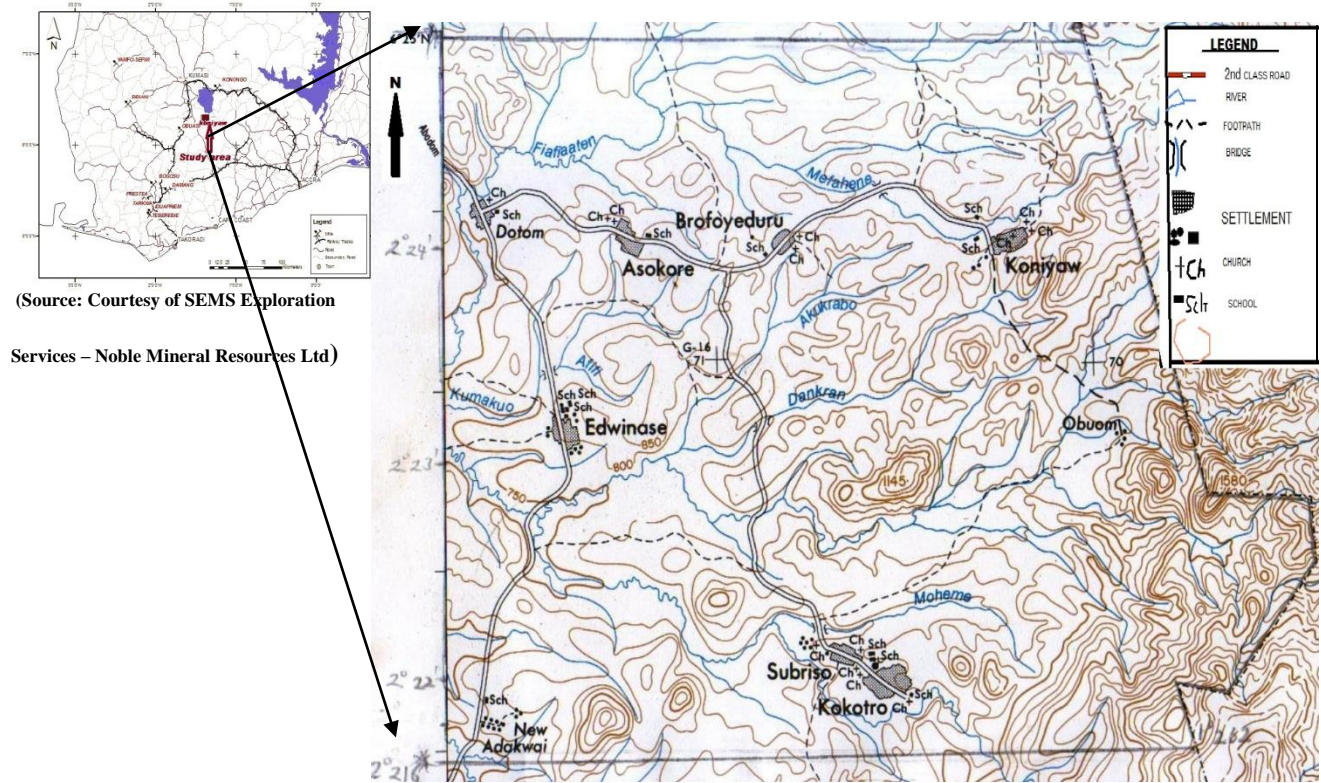
It is hoped that the study would also contribute to the importance of alteration patterns to the interpretation of “Birimian” tectonic settings and relationships rocks have to one another especially these smaller ore bodies that have been separated from these main gold belt zones.

It is strongly believed that the end results of the proposed studies would be of scientific, political, social and economic importance to Ghana.

1.5 LOCATION AND PHYSIOGRAPHY

The study area Koniyaw is found near Bekwai in the Amansie East District. Koniyaw is located between the geographical coordinates in Degree Minutes Seconds (WGS84) is of latitude 6°25’N and 6°21’45”N and longitude 1°25E and 1.26’15”E, and in the southern part Kumasi in the Ashanti Region of Ghana (Figure 1). The Bekwai Municipal district covers a land area of about 709.4 km² with a population size of 18,397 that of Koniyaw being about 1,731 (Ghana Statistical Survey, 2012).

The climate is of the semi-equatorial type with a double maxima rainfall regime. Mean annual rainfall ranges between 1600mm to 1800mm. Average annual temperature is 25.5°C and relative humidity is 75% - 80% in the wet season. The vegetation is predominantly a semi-deciduous forest type with tree canopies and has an elevation of 220m above sea level. The temperature may drop as low as 21⁰C (Ghana Meteorological Service Department, 2004). Relative humidity is fairly moderate but high during the rainy season.



(Source: Courtesy of SEMS Exploration Services – Noble Mineral Resources Ltd)

Fig.1.1 Physiological map of Study area

The study area which is part of field sheet 0602D1 with a scale of 1:50,000 is very close to the Bosomtwe Lake of the Ashanti Region. The study area and its environs are less developed hence is characterized by relatively bad road of third class which does not provide easy access to the study area. At places where footpaths were used, it required walking on sloping lands with great care and concern. The presence of a telecommunication network bridged the communication gap between the towns and other major towns. Basically, the means of transport of the natives were by trosky and walking.

The Dankran stream drains the area in N-S and NE-SW directions respectively. It has its source from the mountains of the 'Obuem' – meaning from rock – and drains through a network of smaller streams, while the dotom drains some abandoned open pit areas.

The vegetation of the area is within the moist semi-deciduous forest zone which is associated with high temperatures and heavy rainfall promoting plants growth. There is no resting periods for the plants and flowering, fruition and shedding of leaves go on side by side (Dickson and Benneh, 1995). However, human activities, particularly farming, timber extraction and small scale mining have reduced the primary forest to secondary forests.

The rain forest consist of three layers of trees referred the upper, middle and lower layers. The middle and lowers have more or less continuous canopies and below the lower is found undergrowth with the ground vegetation. The undergrowth consists of low young trees and herbs (Dickson and Benneh, 1995).

The upper tree layer consists of scattered trees between 35 and 45 meters high and has very wide crowns. The trees of the middle layer are between 15 and 35 meters high and generally have narrow crowns. The lower tree layer consists of numerous trees with narrow closely packed crowns and trees are between 10 and 15 meters high (Dickson and Benneh, 1995).

The soils found in this area are forest oxysols. The colour of the soil ranges from brown to orange and are porous, well-drained and generally loamy. Due to the type of rainfall experience in this area, leaching of certain minerals has made the soil acidic (Dickson and Benneh, 1995).

1.6 HISTORY

The Obuem Mine concession is located at latitude 6°23'26"N and longitude 1°26'14"E (WGS84 geographical coordinates) in the Ashanti Region of Ghana. Important discoveries made in 1930s on the Obuasi fissure resulted in further exploration by other colonial geologist on the Konongo-Axim Belt. These lead to the discovery of the Obuem Gold Mines in 1935. The concession was renamed Obuem Mine concession after being nationalized in 1972 and in 1978 mining activities recommenced as the mine was developed and operated by upon by foreign investors. Commercial gold production commenced at Obuem in the early 1980s by one foreign investor G. D. Peters and was suspended in 1995.

In the late 1990s and early 2000, one Mr. Ankra acquired various rights to the old Obuem mine, renamed it to Koniyaw-Obuem Gold mine and embarked on separate tailings reclamation and surface exploration programmes. The surface exploration programme resulted in the delineation of an open pit resource and a positive feasibility study. In the mid-2000 a new right was obtained by Ossibob Mining Company Ltd. But was separated and shared among co-founders of the company.

The results of further explorations gave grounds for considerable hopefulness and justified resourcing for an increase in output (Junner, 1932). In 1938 plans were then made by these English folks on Mine Development, concentrated on sinking new shafts, connect all shafts and begin a large-scale production.

Despite the country's gold potential, it had been unable to attract any major foreign investment or participation since 1942. Many mines that had opened during the second "jungle boom" (an African post-war equivalent of the American gold rushes) had closed down and many exploration ventures were postponed of which was no exception.

This situation has hindered the acquisition of detailed petrographic work and studies that would have been the foundation or basis for further exploration work.

The Minerals Commission granted a small scale gold mining concession comprising 24 acres (0.097sq.km) on August 2010 in respect of an area immediately surrounding the old Obuem mines shaft to Nana Apraku Small Scale Mining for 2 years renewable. Since then the main Obuem mine concession is owned by Nana Apraku where most mining works are that of a small scale regime. There are other small scale miners as Agya Adom & Sons, among others who also re-worked the ground surface to recover gold remnants in lower concentrations.

It is of these modern times that researchers are focusing on conducting geological mapping and studies to acquire and ascertain the in-situ spatial relationship among host rock, of which this research forms part.

CHAPTER TWO

2.0 LITERATURE REVIEW

2.1 GLOBAL GEOLOGY

The Precambrian shield of West Africa embraces the Archaean-Proterozoic from 3.8 – 1.8 Ga WAC (Kouamelan et al., 1997) and it's rejuvenated Pan African Belts and regions. The craton is bounded to the East and West by Pan African Mobile Belts.

The West African craton has remained tectonically stable since about 2.0 Ga (Attoh et. al., 1997). Two craton-wide geochrono-lithotectonic provinces can be distinguished that subdivide the West African Craton fairly longitudinally into;

- i) The late Archaean Province (3.8 – 2.6 Ga) ago to the West
- ii) The Proterozoic Province east 2.2 – 1.9 Ga (Kouamelan et. al., 1997)

The Archaean rocks are represented largely by grey-gneisses, migmatitic orthogneisses and magmatic complexes of metamorphosed to amphibolite and granulite facies. Allibone et al. (2002a) concluded that the “Eoeburnean” events are characterized by Supracrustal metasedimentary and metavolcanic rocks, greenstones and granites (Fig. 2.1a). These rocks were affected by and record evidences of major later orogenic events dated at 3000 and 2800 Ma ago (Attoh et al., 1997).

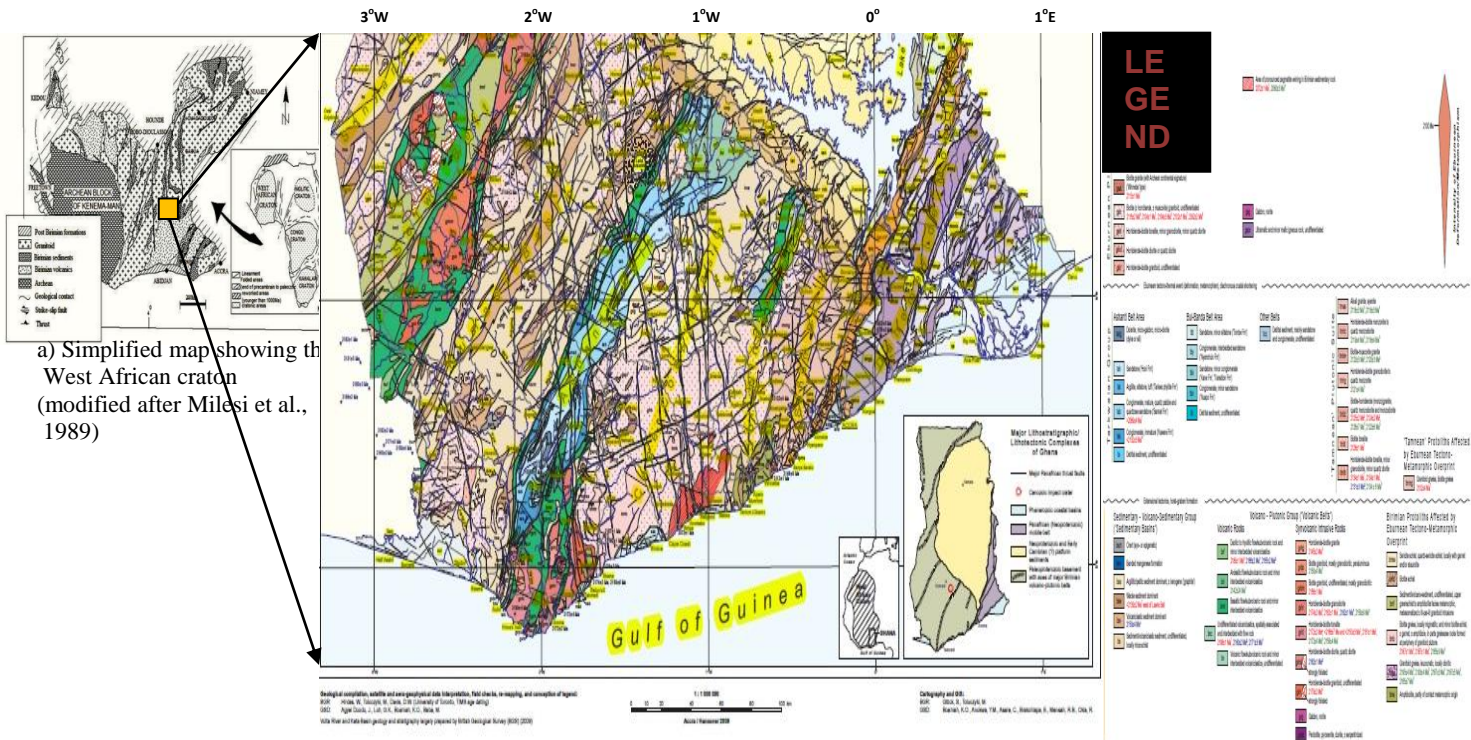
Feybesse et al. (2006) proposed an early Eburnean phase between 2135 Ma and 2100 Ma corresponding to magmatic accretion and plutonism that terminated with development of the Kumasi Basin. The synchronous Eburnean orogeny (2130–1980 Ma) corresponds to thrust tectonism dominated by sinistral transcurrent deformation in the Ashanti Belt.

Allibone et al. (2002a) suggest an alternative two phase Eburnean evolution, divided into the Eburnean I (2200 – 2150 Ma) and Eburnean II (2116 – 2088 Ma), that are separated by deposition of the Birimian and Tarkwaian units. This was also known in northern Ghana as Eoeburnean and Eburnean, respectively (De Kock et al., 2011).

The Eburnean I (Eoeburnean) event was associated with a period of magmatism and metamorphism responsible for the Sefwi Group metavolcanics (Allibone et al., 2002a) and TTG granitoid emplacement that correlates with the pre-Eburnean of Feybesse et al. (2006).

The Eburnean II (Eburnean) event is associated with major NW-SE shortening (D2 of Allibone et al. (2002a, b); D1 of Tunks et al. (2004)) that developed major thrust faults – including the Ashanti Fault – along with isoclinal folds in Birimian metasediments and regional scale open folds in the Tarkwaian sediments (Fig. 2.1b).

The second phase of the Eburnean orogeny affects both the Tarkwaian group and the Birimian Supergroup after 2133 ± 4 Ma. The features of thrust overprints were reactivated during a phase of sinistral transgression that exploits the previously occurring thrusts (Feybesse et. al., 2006)



a) Simplified map showing the West African craton (modified after Milesi et al., 1989)

b) Birimian volcanic and sedimentary rocks define the regional-scale geological rocks in southwestern Ghana (After GSD of Ghana & BGR of Germany, 2009).

Fig.2.1 Regional geology of southwestern Ghana.

2.2 BIRIMIAN GEOLOGY (REGIONAL GEOLOGY)

A characteristic feature of the Ashanti belt, as compared to other Birimian volcanic belts in Ghana, is the predominance of volcanoclastic rocks and the relatively sparse development of lava flows. This, in conjunction with the almost complete preservation of the overlying Tarkwaian rocks, suggests that the Ashanti belt represents a crustal segment characterized by a relatively shallow erosion level (Leube & Hirdes, 1986). All volcanic rocks in the project area and their subvolcanic equivalents occur in the Ashanti volcanic belt

Bessoles (1977) disagreeing with the presence of eugeosynclines, miogeosynclines and ophiolites -distinguished the following two units instead:

- Type 1 units which were said to have been deposited in deep troughs with high length/width ratios, and to consist of greenstones, metabasalts, volcanoclastic rocks, quartzites, phyllites, and gneisses, overlain by flysch-type sediments.
- Type 2 units were said to have been laid down in broad shallow basins and to be composed of predominantly felsic volcanosedimentary sequences, sericite schists, greywackes, quartzites, meta-conglomerates and calc-chlorite schists, with greenstones and flysch being practically absent.

Vidal et al. (1992) suggested that "the upper Birimian (B 2) mafic volcanics" rest on pre-existing, continental (Dabakalian or B 1) basement. Abouchami et al. (1990) and Boher et al. (1992), on the other hand, noted the lack of evidence for inherited Archean or very early Proterozoic crust in the central and eastern parts of the craton, as well as the juvenile character of Birimian tholeiitic basalts. The latter authors accepted the existence of two Paleoproterozoic cycles (Burkinian and Birimian), however, and proposed that the first took place between 2.2 and 2.15 Ga, and the second between 2.12 and 2.07 Ga.

Hirdes & Leube (1989) pointed out that gold mineralization in Birimian rocks in Ghana is strikingly concentrated in 10-15 km wide corridors along volcanic belt/sedimentary basin boundaries, and ascribed this phenomenon to the presence of chemical sediments as well as widespread and intensive tectonization in the belt/basin transition zones.

In brief, the above authors suggested an evolution of the tectonic setting of the Birimian/Eburnean in Ghana from an intracratonic-rift to oceanic-spreading and finally to an accretion-collision-related setting.

2.3 LOCAL GEOLOGY

The Obuem mine concession is found in the southern part of the Ashanti Region of Ghana and the basement rocks are early Proterozoic in age. The geology is mainly composed of Birimian rocks, which have been dated at 2.0 – 2.3 Ma (Taylor et al., 1992). These rocks are mainly composed of metamorphosed volcanic rocks and sediments (Fig.2.2).

Outcrops within this concession are exposed within pits that were dug by illegal small-scale miners and also in the deep pits by Gold Coast miners around the Second World War. Mapping of this concession shows lithologies that have been divided into 3 distinct groups.

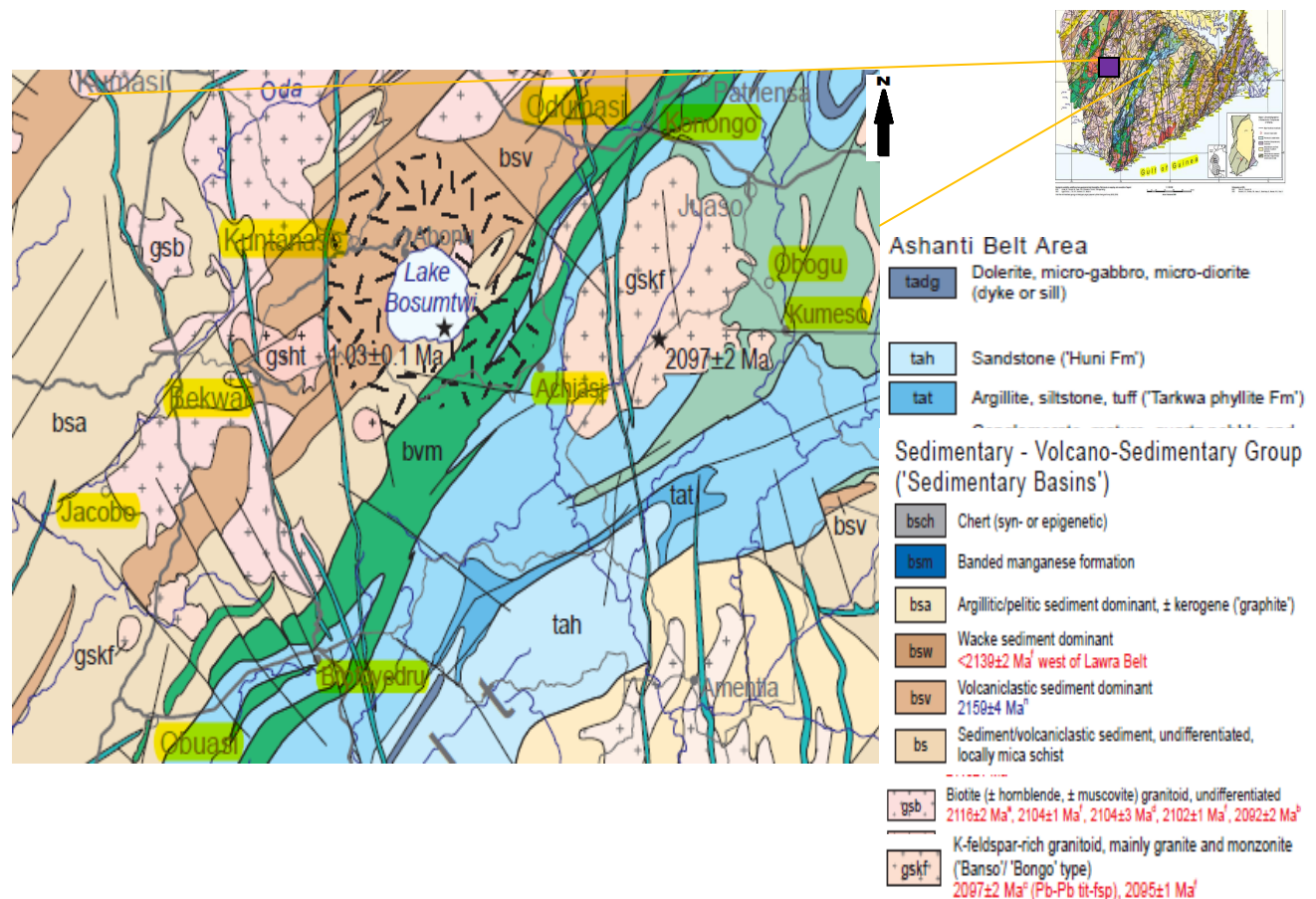


Fig.2.2 Geology of Study area. Birimian volcanic and sedimentary rocks define the regional-scale geological rocks in southwestern Ghana (After GSD of Ghana & BGR of Germany, 2009).

- Type 1 units which consist of greenstones, metabasalt and volcanoclastic rocks.
- Type 2 units composed of predominantly felsic volcanosedimentary sequences, meta-schists, greywackes, phyllites and quartzites. (Bessoles, 1977).
- Type 3 rocks of volcanic intrusive comprising of granitoids and granodiorite.

The Birimian metavolcanics in the South Ashanti Belt are composed of tholeiitic basalts, which are generally massive. The rock units show a general NNE-SSW trend (Fig 2.2). The belt-type intrusive complexes are dominantly granodiorite in composition but in some phases are characterized by high radiometric potassium content (Griff, 1998). The belt-type granitoids in this study area rarely show any evidence of foliation, even near the contacts with volcanic rocks. Supracrustal and intrusive rocks of the 2150-2185 Ma time span are at least locally present as various gneisses which previously had been termed "Dabakalian" (Hirdes et al. 1992).

Late Eburnean deformation has been observed at Kokotro near Obuem mines with visible and outstretched minor foldings. The third deformation diagram of Tunks et al., (2004) corresponds to SE – NW shortening connected with folds quartz veins and a shallow dipping crenulations cleavage that overprints the reactivated thrust faults.

CHAPTER THREE

3.0 METHODOLOGY

3.1 INTRODUCTION

This section provides the background knowledge about how this research was carried out. Analytical studies in terms of mineralogy, petrology and structures were conducted for in depth understanding of geospatial field relation. These activities are performed in an orderly methodical fashion and will be discussed in the next section summarised into pre-field work, field work and post field work.

3.1.1 PRE-FIELD WORK

Relevant literature materials were collected and studied on the formation and general geology of the area. The base map for the study area was obtained from the Geological Survey of Ghana and the coordinates of the study area noted. Further academic studies were made on mineralogy, petrology and structures on the area of which the concession was found for thorough understanding of the field terrane. These provided the significant background knowledge which facilitated the field investigation.

3.1.2 FIELD WORK

Reconnaissance survey was taken to have a general idea of the topography, accessibility and possible outcrop locations in the study area. This included traversing all the accessible parts of the area under study, including streams, roads, footpaths and even areas which were inaccessible. This was the moment where most field kits and instruments such as the Garmin GPS, compass, digital pace counter, were reset and geological hammer, dilute HCl, etc, tested before the actual field work begin. The geological compass used was corrected to a declination of 4⁰W of the

geographical north ensuring that the compass north coincided with the north indicator of the base map. The mapping was done with the survey map of Ghana field sheet number 0602D1 with scale of 1:50,000.

Field mapping involved activities such as pace and compass traversing, taking GPS reading of pits and outcrops location, describing rocks found in the area, taking attitudes of the different structural elements of the rocks found in the area, recording data in field note books and on overlays and taking oriented samples of rocks in the area.

The mapping was done by using the Garmin GPS to measure distances and directions and the citing and pacing method was used to support the bearings or directions of the GPS. The pace and compass method was also used in calculating the length and width of outcrops. This is done by walking the outcrop's length and width. Other equipment like hammer, a hand lens, diluted HCl, cutlass and sample bags were also utilized to chip rocks, view minerals in hand specimen, test the presence of carbonaceous minerals, clear foot paths and contain rock samples respectively on the field.

In the cause of the field work several observations were made. Geologic mapping was undertaken in all the accessible outcrops and pits at the Obuem concession and throughout the surrounding area (Fig.3.1). The bearings recorded along with the distances measured are used in plotting the positions and bearing of outcrops located in the field on their respective overlays. Structural and geometric measurements were taken using the geological compass and surveyors tape (if possible) respectively. Rock samples were processed in the laboratories by cutting and polishing of thin sections and pictures taken were digitized and keenly observed.

Most measurements done in the field are of two types. The main attitudes measured are the strike and dip of joints surfaces as well as the trend and plunge of 3-D fold structures. The strike and

trend are measured with the aid of the compass needle and the bull's eye level on the geological compass. The dip and plunge on the other hand are measured using the clinometers on the geological compass.



Fig.3.1 Photographs of some sample locations of rocks (for geochemical analysis. Photographs were taken almost standing vertical

Lithological sampling was done taking into consideration several factors. Sampling is done only from fresh surfaces of the rock. Oriented samples from the in-situ rocks with their measured strike and dip recorded on them were taken. The samples were large enough to be representative of all the mineralogical and structural features of the outcrops from which they are taken. Samples were also taken from dug pits both from previous mine tunnels and that from small scale miners. The sample stations were and their positions were marked with the GPS.

All rocks in the field were thoroughly described. This include describing the Color, Grain size, Minerals seen identified, Indurations, Structures found, Weathering and Field location and name. The various rock outcrops were all given station numbers. These station numbers serve as the names of the outcrops and make it easier to identify which outcrop contains what features. Traverse, structural and outcrop data obtained from the field are also plotted on the GPS. Plotting was done using the map's scale alongside the data to be plotted. This aids in the correct plotting of the location and trend of the different data to be plotted.

3.1.3 POST FIELD WORK

3.3.1 Petrology

The samples for this study were taken from the Obuem concession and areas surrounding the mines which fall within the Birimian terrane recognised in Ghana. Oriented samples taken were categorised according to the three main rock types before taken to the Department of Earth Science Laboratory to prepare them for thin section studies. Petrological summary of the samples

gives an indication that most of the rocks most likely originated from a mafic igneous or have igneous protoliths. Metasediments found within mine pits at the Obuem mine site still shows megascopic features of metamorphism probably regional. Hand specimen samples were described in terms of colour, texture, visible deformation features, and then photographed. The method used to process, organise and visualize results are also discussed.

3.3.2 Preparation of Thin Section analysis

Thin sections of 29 rock samples were made of samples from the Obuem concession and surrounding areas. Later petrographical and microstructural analyses were done in the Department of Earth Science at the University of Ghana Campus. The following is a summarized procedure of how thin sections of the selected rock samples was prepared.

A thin slice (a few millimeters thick) was cut from the specimen using a diamond saw ensuring the cut is perpendicular to any planar fabric present in the rock. The slice was grounded flat and smooth on one surface using progressively finer abrasive to a thickness of about 30 μ m. The smooth surface was cemented to glass slide (2'' x 1'') using Canada balsam cement and heated using a laboratory gas burner. Progressively finer abrasives were used as the section became thinner, and finishing was done with 600-grade carborundum powder. The thickness was gauged by observing the interference colours of common minerals such as quartz or feldspar. After cleaning excess cement from the section, it was covered with a glass cover-slip cemented on with Canada balsam ensuring that air bubbles were expelled from the section.

These thin sections were examined using the Optical Electronic microscope for petrographical and microstructural analyses. Textural features such as grain sizes, grain orientation, grain boundary, mineralogical composition were studied. Observations made are shown under results.

3.3.3 Geochemical analysis

A total of 25 samples were geochemically analyzed for 13 major elements (SiO₂, Al₂O₃, total Fe as Fe₂O₃, CaO, MgO, Na₂O, K₂O, P₂O₅, SrO, MnO, TiO₂, MnO, P₂O₅, SrO, and BaO) and 31 minor and trace elements (Nb, Zr, Y, Sr, Rb, Sc, V, Cr, Ni, Cu, Zn, Ba, La, Ce, Pr, Nd, Eu, Sm, Gd, Tb, Dy, Ho, Er, Li, Yb, Lu, Hf, Ta, Pb, Th, and U) by ALS Minerals, Vancouver Laboratory through the ALS Chemex Ghana Limited. Whole Rock Package analysis was done to determine the major elements using X-ray fluorescence – XRF. Minor and trace elements were determined by aqua regia method of Inductively Coupled Plasma Mass Spectroscopy (ICPMS). The concentrations of rare earth elements (REE) and other trace elements in whole rock were also determined using ICPMS acid digestion techniques. Through this method the percentage by composition of the main oxides is established as well as the trace elements. The XRF method was chosen because it is economic and efficient. Crucible heating method was carried out to measure the moisture contents of the samples (loss to ignition).

To check for quality control two blanks and standards were added to the samples. Details of the analytical procedure and methods in terms of accuracy, precision and standards can be found in the brochure of ALS Minerals Schedule of Fees and Services. Interpretation of the geochemical was done with the aid of some geological software.

CHAPTER FOUR

4.0 RESULTS

4.1 PETROGRAPHY

4.1. 1 Granitoids

From hand specimen observation, prominent appearance of darker minerals gives the rock darker or mafic colour. In general rock shows granitic crystal aggregates of phaneritic texture with large visible holocrystalline crystals. Hornblende and biotite make up the mafic crystals and the light colored crystals compromise the plagioclase feldspar, Quartz and K-feldspar (Fig.4.1 b). No significant deformation or degree of metamorphism is seen in hand specimen.

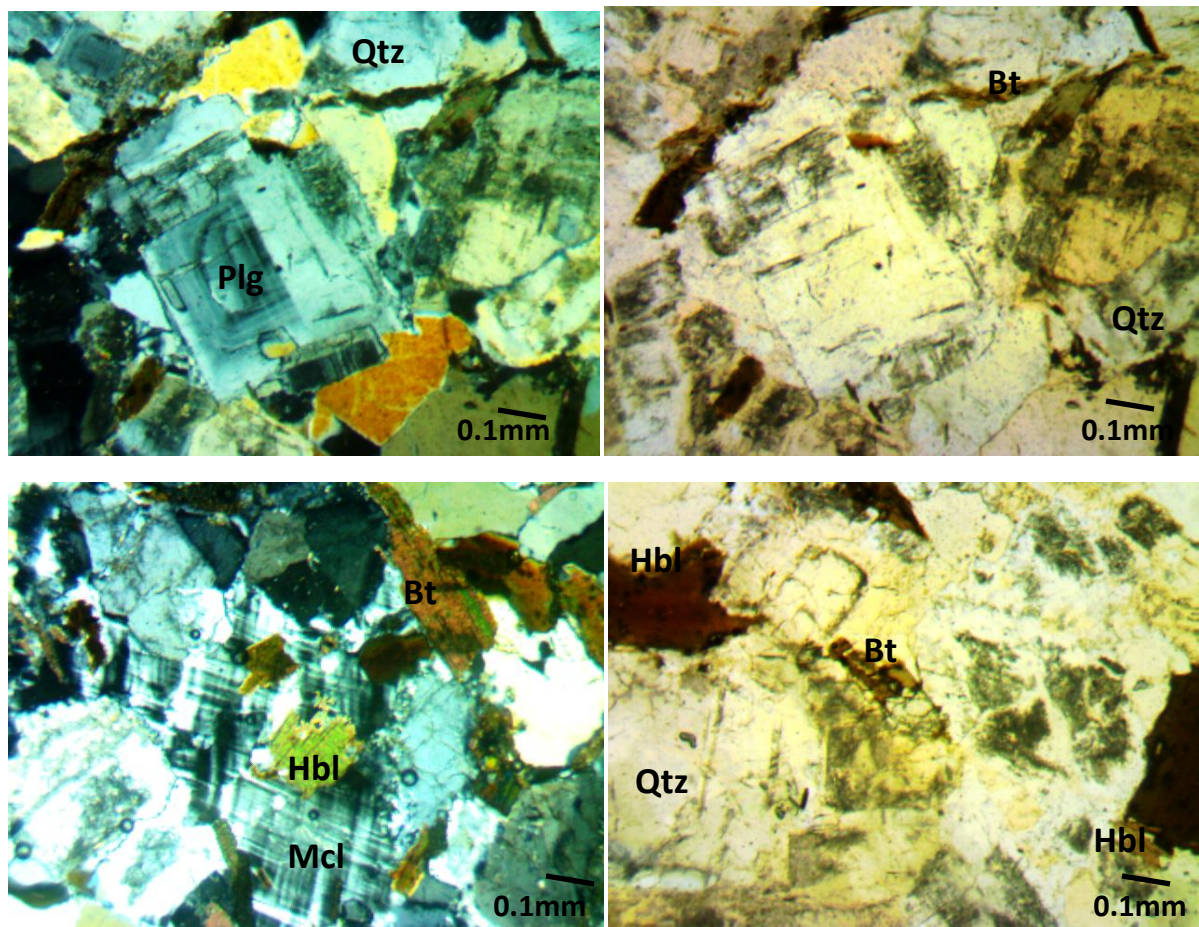


a)

b)

Fig.4.1 Photograph of a Granitic Boulder at Gyasikrom. (Photograph taken facing the south).

From thin section studies, the rocks show a medium to coarse-grained subhedral granular texture. Well formed crystals of Plagioclase feldspar, quartz and Alkaline Feldspar constitute the majority of or are the predominant mineral phases. Though in hand specimen biotite, muscovite and hornblende appear to be the most prominent, their percentage in thin section indicates they are not but then form the dominant mafic phase (Fig.4.2).



a.

b.

Fig. 4.2 Photomicrograph of Granite rock in both a. Crossed nicols and b. plane polarized light. (Mineral symbols: Plg = Plagioclase, Mcl = Microcline, Qtz = Quartz, Bt = biotite; Mcl = microcline; Hbl = Hornblende)

Table 1

Representative compositions of major minerals in the Granitoids.

Mineral	Percentage	Characteristics
Quartz	30%	They show weak undulose extinction and mostly have cracks. The crystal structure seems to be deformed due to strain on grain contacts resulting in vertical shortening of grain contacts. They appear to be ‘squashed’ or crushed into pieces and form within the interstitial spaces of almost all the minerals. Strain has caused the quartz crystal to deform into domains with slightly different extinction angles. The quartz lacks alteration and no inclusions were seen.
Plagioclase Feldspar	25%	More or less equant euhedral to subhedral tabular crystals. They are white or gray lath-shaped grains with subhedral rectangular shapes. Most show albite twinning with few patches of crosshatched twinning in the cores of crystals. The plagioclases are more altered than the alkali feldspar and slightly higher

		relief. They show alteration into sericite along cracks and edges
Alkali Feldspar	10%	They also have distortions in the originally white and/or pink lath-shaped and seem some have been crushed.
Muscovite	8%	The Muscovites are anhedral to subhedral crystals and are in contacts with quartz crystals.
Biotite	12%	The flat, flaky grains with dark brown colour and cleavage in one direction have cracks and some alteration into sericite.
Hornblende	12%	The hornblende crystals are usually prismatic and are irregular in outline, wrapping round the feldspar and quartz.
Other Accessory	3%	Appears to be dark or opaque both under cross and plane polars. Opaque (believe to be Fe-bearing oxide - ilmenite or magnetite) are seen to form a long grain boundaries cracks of the Biotite and hornblende.

4.1.2 Metasediments

The metasediments seen on the field are mainly metamorphosed phyllites, schist and metagreywackes.

1. Phyllites

Megascopically, the phyllites have fine grained platy mineral probably consisting mainly of sericite. The phyllites are fine grained, but have lustrous sheen on both the strongly and thinly foliated surfaces. The rocks show some evidence of ductile deformation by breaking along foliation planes but it is also friable.

Two forms of phyllites were encountered. These are the evenly foliated brown to grey phyllites (Fig.4.3a) and the graphitic phyllites which are black and have silky luster (Fig.4.3a) . The former is somehow harder than the later which is very fine grained and splits easily into thin or even powdery because of its smooth slaty foliation.

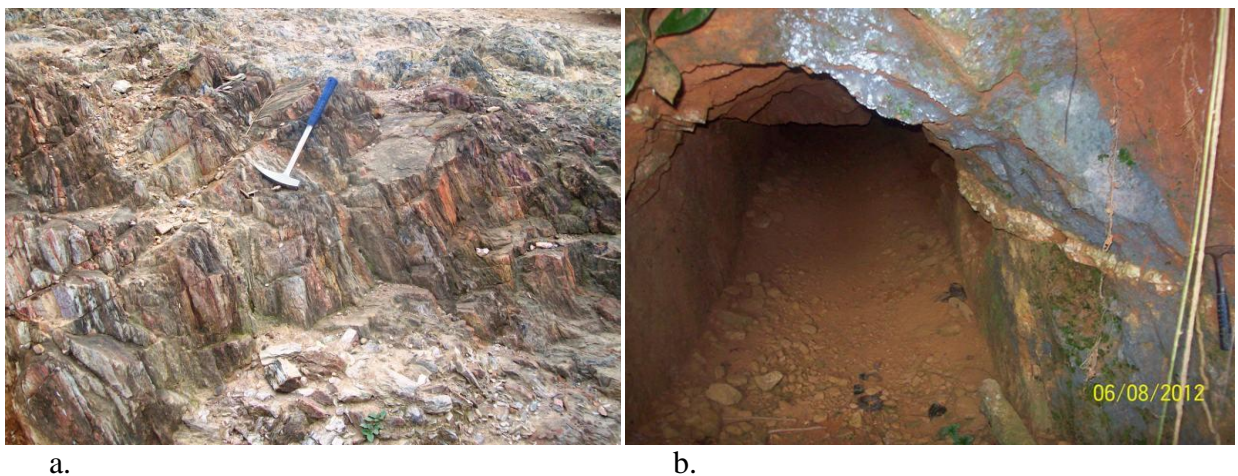


Fig.4.3 (a) Photograph of massive, jointed and veined Phyllites at Kokotro (b) Graphitic Phyllites at Obuem Mine. Photograph taken facing the North

The phyllites show some degree of weathering with the production of clay. The phyllites appear to be more siliceous and most of them are pelitic and may probably suggest a shale or mudstone protoliths.

2. Schist

For the metamorphosed schist, it has medium to coarse grained texture, the fabric of which is characterized by an excellent parallelism or schistosity. The individual mineral grains could be recognized megascopically (Fig.4.3a). Towards Kokotro the grey colour of schist turns to show a greenish colour probably because of the presence of chlorite mineral.

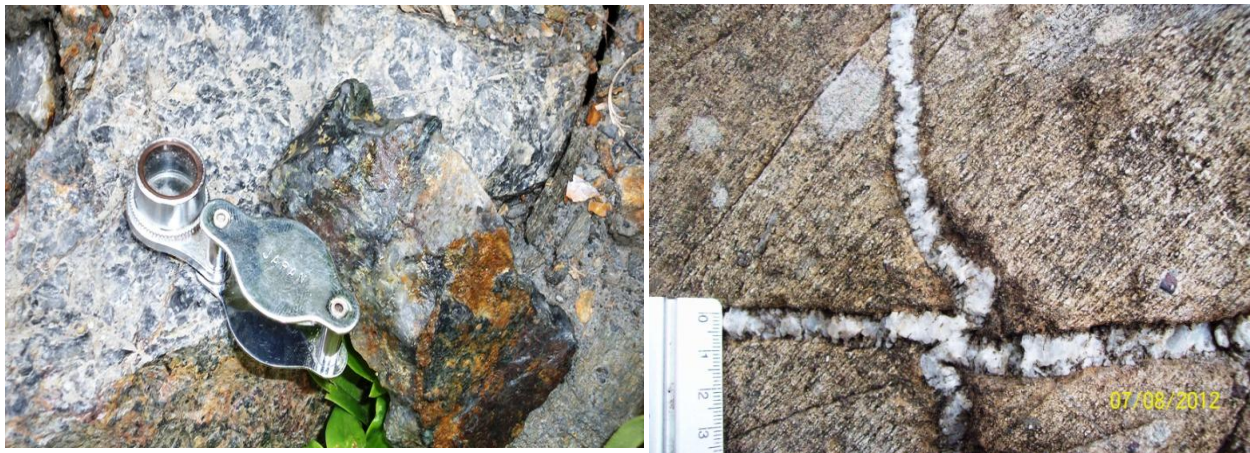


Fig.4.4 Photograph of massive and veined Schist at Subriso. Photograph taken facing the North

Table 2

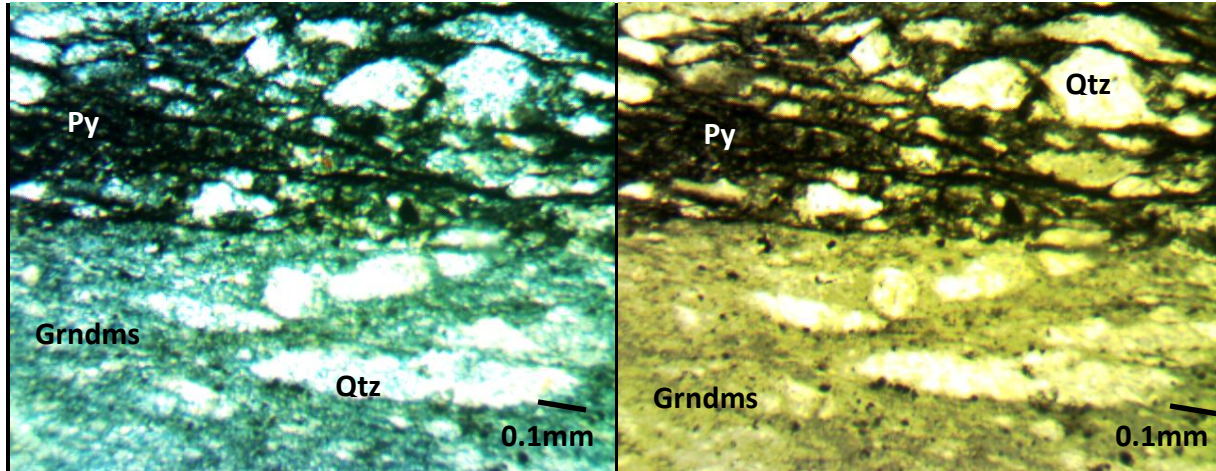
Representative compositions of major minerals from the metasediments.

MINERAL	Phyllites		Schist	
	VOLUME (in %)	CHARACTERISTIC FEATURES	VOLUME (in %)	CHARACTERISTIC FEATURES
Feldspar	10%	Crushed pieces of anhedral Feldspars Grains with distortions in the originally white and/or pink lath-shaped mineral.	15%	Grains are anhedral and have distortions in the originally white and/or pink lath-shaped mineral. Feldspars look as if they have been crushed into pieces.
Quartz	15%	They appear to have interstitial, poorly defined grains. It also shows no zoning.	40%	They appear to have interstitial, poorly defined grains. It also shows no zoning, low relief and low birefringence.
Muscovite	10%	Minerals seem to have a preferred orientation Some grains have merged with neighbouring minerals in contact.	25%	They have a mottled-shape appearance and show a very slight greenish to pale yellow tint. Some grains have been welded into their neighbours or penetrating them slightly. Minerals seem to have a preferred orientation

Chlorite	5%	Chlorite showing interference (light grey-green) colours are intergrown with feldspar resulting in banding. Occurring across the foliation.	20%	They show colourless or a little green anhedral to subhedral shape and have a perfect cleavage in one direction. Some of them are intergrown with k-feldspar and some are seen adjacent to mostly altered biotite.
Graphite	15%	These form bands which intercalate with quartz and mica.		
Groundmass	40%	The mica groundmass have a bend edges and realigned and alternate with the phenocrysts. They are stretched.	10%	These are mostly made up of mixed compositions of weathered grains of micas, quartz and feldspars. They turned to occupy the boundary and margins between phenocrysts.
Accessory mineral	5%	These minerals are epidote and Fe-rich mineral that might be chlorite or sericite	2%	Appears to be dark or opaque both under cross and plane polar. Opaque (believe to be Fe-bearing oxide - ilmenite or magnetite)

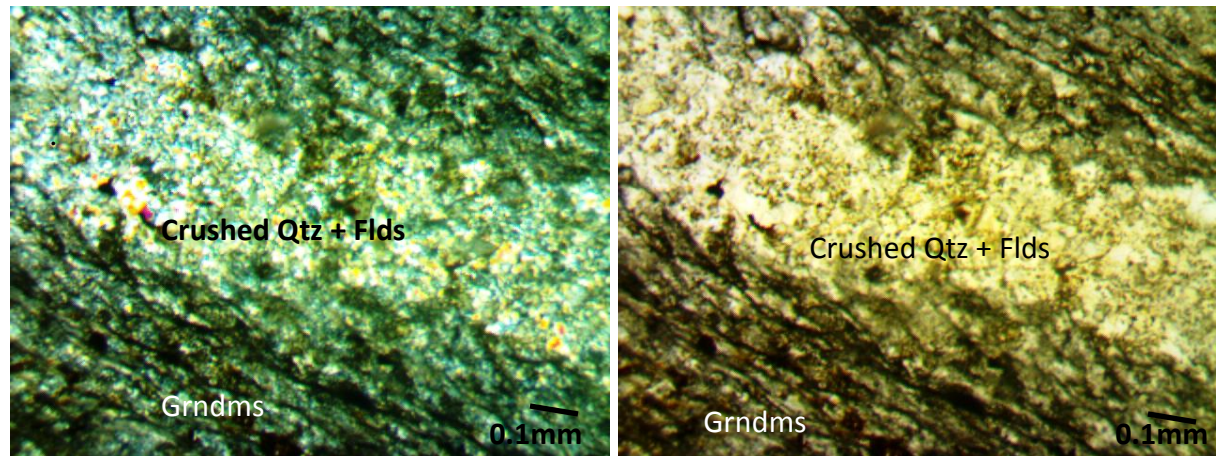
Thin section observation of the Phyllite rocks (Fig.4.5) shows more than 30 per cent of clay and easily destroyed minerals. Though the rock is made up of mixed minerals and rock fragments, the major minerals (phenocrysts) seen are mainly micaceous muscovite and broken quartz crystals. Others may include scanty accessory minerals of some ferromagnesian minerals (Table 2). Under the microscope the rock exhibits micro-foliations due to alignment of mineral grains (preferred orientation of the mica in Fig.4.5b). It was revealed that the grains have been reduced (crushed).

The ground mass is also made up of argillaceous (fine grained rock dust) fragments which is a bit difficult to decipher but may be from the decomposition product of the mica, some feldspars and chlorite matter (Fig.4.5 a and b). These ground mass is cemented with iron oxide that may be responsible for the faint brown colour of some grains.



a1

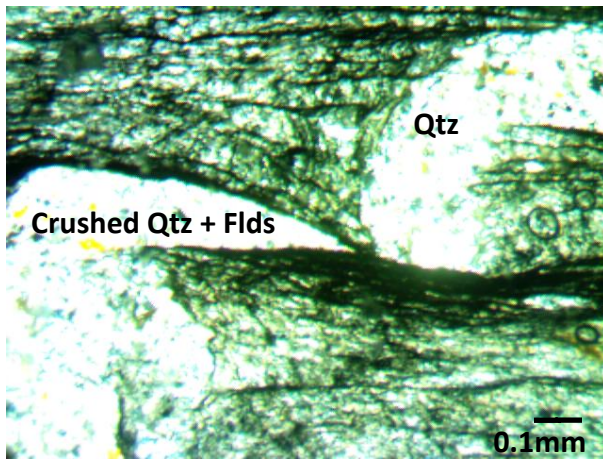
a2



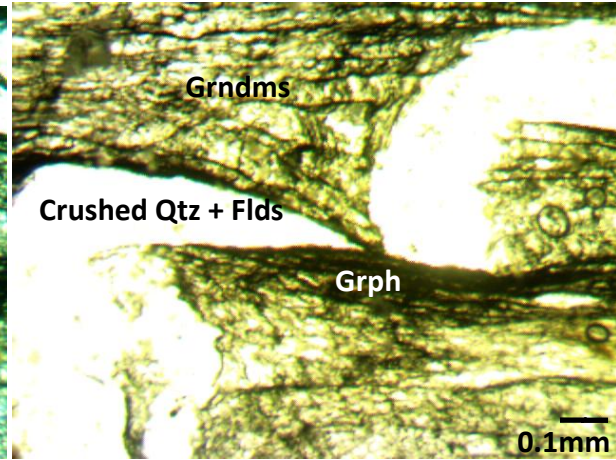
b1

b2

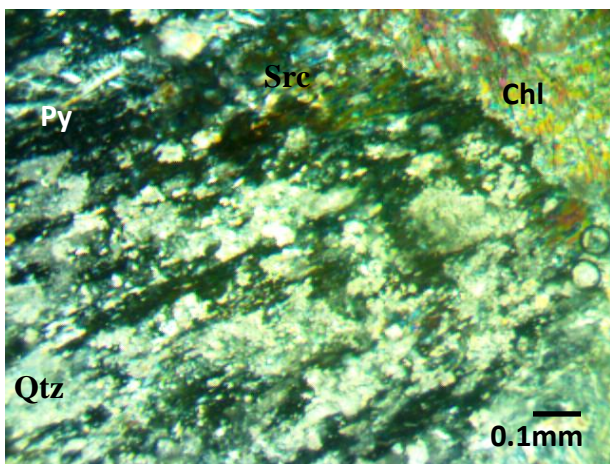
Fig.4.5 Photomicrograph of a crenulated Graphitic Phyllite (a) and crenulated Normal Phyllite (b) both in Crossed nicols(a1 and b1) and plane polarized light (a2 and b2). (Mineral symbols: Flds = Feldspar, Qtz = Quartz, Grndms = Groundmass, Py = Pyrite;)



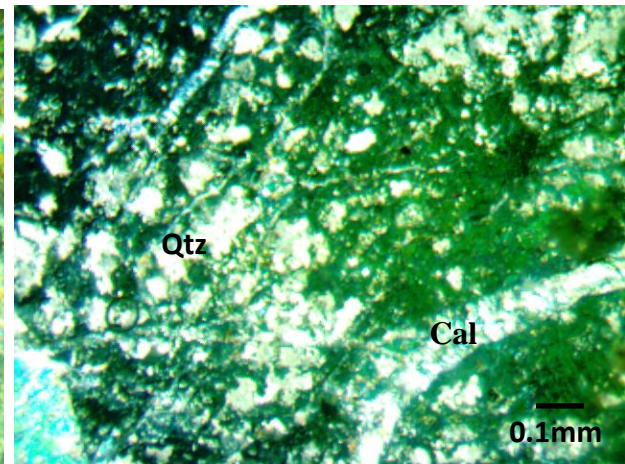
a1.



a2.



b.



c.

Fig. 4.6 Photomicrograph of a foliated Chlorite Schist both in Crossed nicols and plane polarized light. (Mineral symbols: Flds = Feldspar, Qtz = Quartz, Grndms = Groundmass, Chl= Chlorite, Src = Sericite, Py= Pyrite, Cal=calcite;)

The textural, mineralogical and structural description of schist under this section is as follows. Mineral grains show evidence of micro-foliations due to preferred orientation of the mica (Fig. 4.6). It is seen that the grains have been crushed. The rock shows higher quartz content coupled with the abundance of clay minerals (Table 2). This could be due the extent of weathering of the rock. The quartz grain exhibits undulose extinction and this indicates deformation (stress) in the rock with increase in temperature and pressure. It also has low relief, low birefringence colour since the maximum interference color is gray and lacks visible twinning and alteration.

Other minerals present include chlorite, micas (muscovite), carbonaceous matter and some iron oxide. Chlorite content is high (about 20%). Under plane polars it shows greenish-blue pleochroism and a subhedral shape (Fig. 4.6). Under cross polars chlorite exhibits a fair relief, weak birefringence, simple twinning and extinction angle of 9 degrees.

3. Greywacke

The greywackes show grey, grained well-indurated and crystalline rock (Fig 4.7). The rock is composed of mixed up grains of easily destroyed minerals of rock fragments. Major framework grains are quartz and feldspars, which together with lithic fragments are cemented in a clayey matrix. No significant deformation or degree of metamorphism is seen in hand specimen.

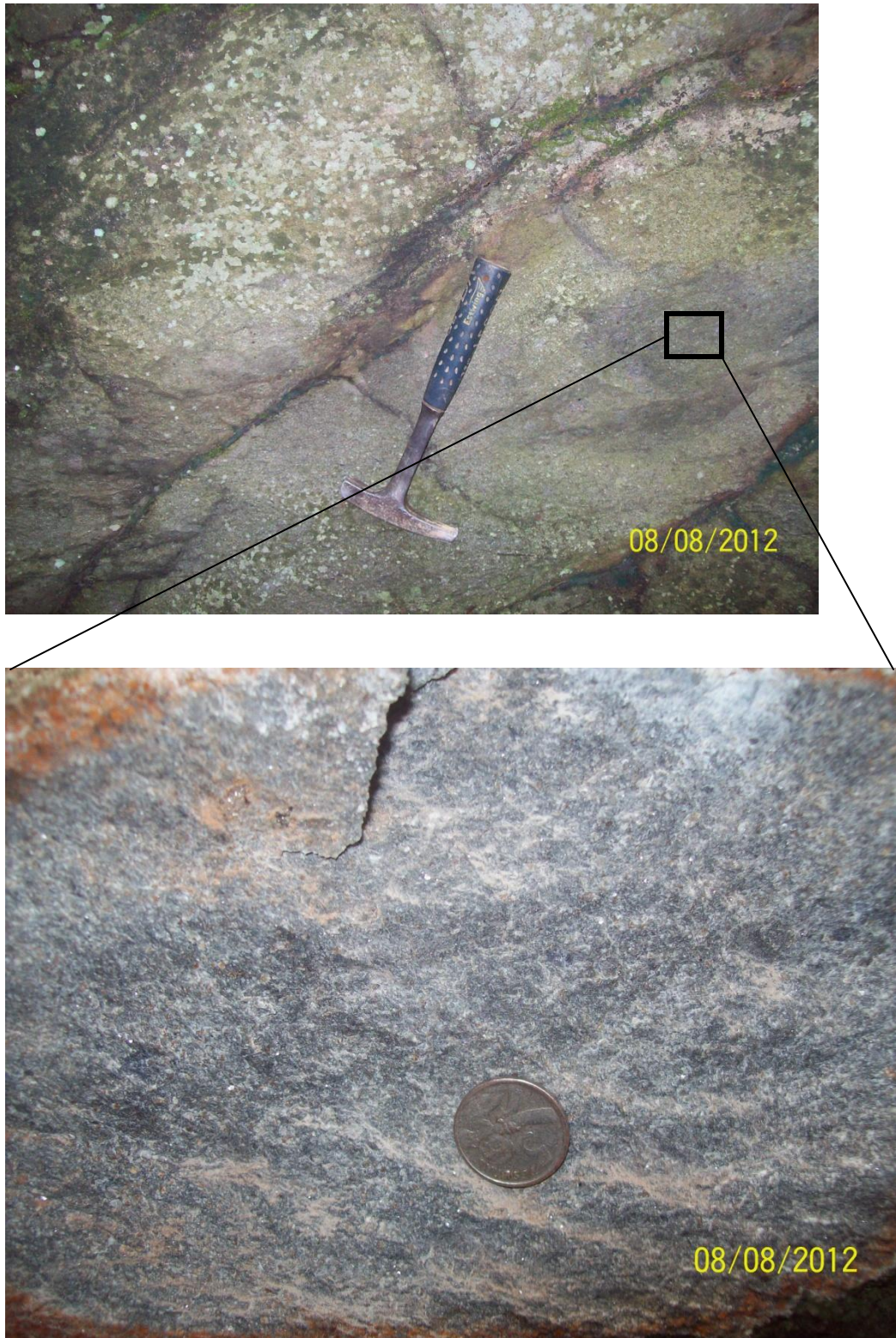
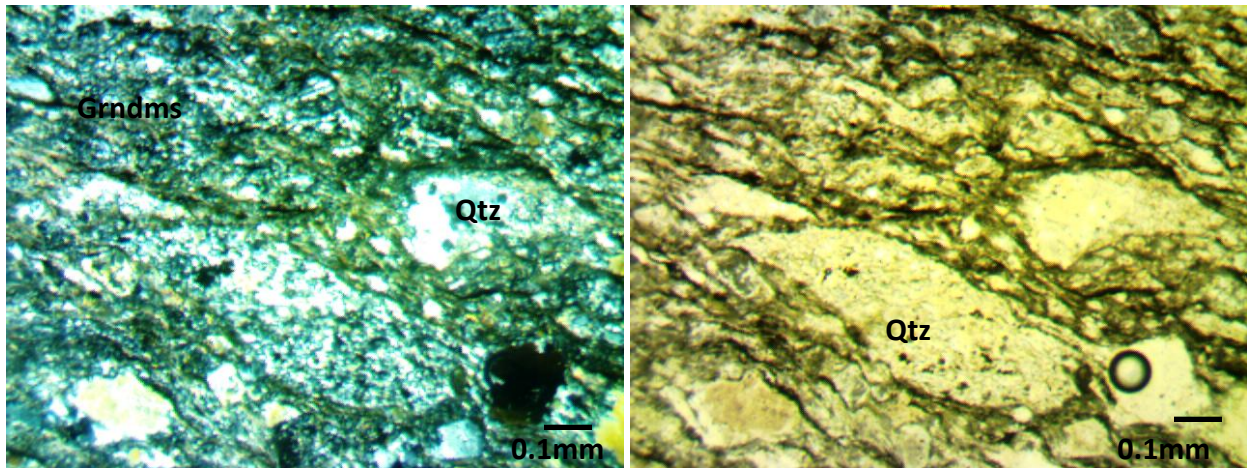
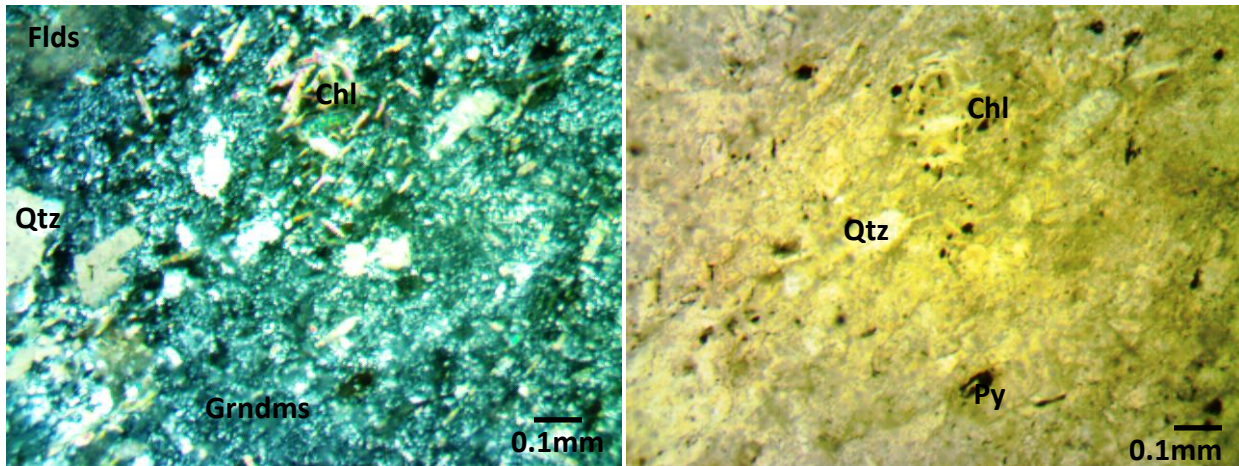


Fig 4.7 Photograph of a Greywacke at Obuem. Photo taken facing South.



a1.

a2.



b1.

b2.

Fig. 4.8 Photomicrograph of a Greywacke both in Crossed nicols (a1 and b1) and plane polarized light (a2 and b2). (Mineral symbols: Flds = Feldspar, Qtz = Quartz, Grndms = Groundmass, Py = Pyrite)

Table 3

Representative compositions of major minerals from the Greywacke.

MINERAL	VOLUME (in %)	CHARACTERISTIC FEATURES
Quartz		
Monocrystalline	30%	Medium grained subhedral crystals with fractures. The quartz lacks alteration and is crushed into pieces at some sections.
Polycrystalline	10%	Medium grained with wavy elongated boundaries that are commonly irregularly sutured.
Feldspar		
Orthoclase	5%	Small, anhedral cloudy grains with distortions in the originally lath-shaped mineral.
Plagioclase	10%	Small, medium grained subhedral crystals with polysynthetic twinning. Grain boundaries not well visible.
Chlorite	5%	Fibrous to threadlike mineral grains that seems to be secondary minerals of mafic minerals alteration.
Rock fragments	12%	These are mostly made up of mixed compositions of fine rock dust or weathered grains of micas, quartz and feldspars. They

		occupy the boundary and margins between phenocrysts and define the foliation.
Matrix (with Cement)	25%	Clayey matrix cemented by a fine rock dust. Matrix is end products of broken and altered framework grains.
Accessory mineral	2%	Alteration product from the feldspars and lithic fragments appears to be chlorite and/or mica.

Thin section of this rock shows a medium grained and a matrix supported epiclastic texture with anhedral to subhedral grains. The rock is poorly to moderately sorted with a subrounded to subangular framework grains of lower sphericity and almost no pore spaces. It is composed of feldspars (plagioclase and Orthoclase) and quartz, making up the framework grains, lithic fragments and a clayey matrix cemented together by a fine rock dust (Fig 4.8).

It shows a high proportion of strained quartz and few altered feldspar and mica grains that lie in a matrix. Broken pieces or microcrystalline quartz, fractures and strain seen in the quartz crystals indicate some form of deformation. The foliation bands are distorted and mainly marked by graphite. The minerals observed have been minutely altered (grain shape and composition). The rock has been moderately compacted and some grains have been welded into their neighbours or penetrating them slightly.

4.1.3 Metavolcanics

The rock has phaneritic texture with hardly visible mineral crystals. Hornblende and biotite make up the mafic crystals and the light colored crystals comprise the feldspar, Quartz and K-feldspar. The rock appears greenish in colour and that might be the presence of chlorite. No significant deformation or degree of metamorphism is seen in hand specimen except for veining (Fig 4.9).



Figure 4.9 Photograph of crystalline and veined metavolcanic rock at Obuem

The thin section shows pyroxene which is altered and shows medium to coarse-grained subhedral granular texture. Well formed crystals of Plagioclase feldspar, quartz and hornblende constitute the majority of the predominant mineral phase (Fig 4.8).

In general the sample is clean, fresh and well crystalline plutonic igneous rock that has not deformed much

Biotite and Amphibole minerals together in hand specimen makes the dark minerals appear to be more prominent than their percentage may indicate in thin section (Fig 4.8), especially in sample two. The clay filling between the quartz grains has been metamorphosed to bright green chlorite.

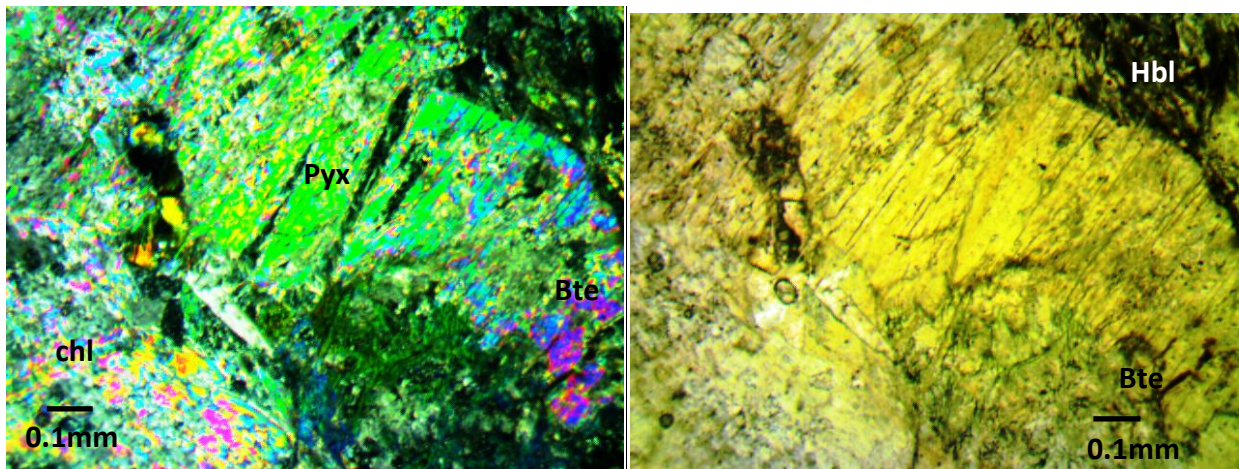


Fig. 4.10 Photomicrograph of a Chlorite-schist both in Crossed nicols and plane polarized light. (Mineral symbols: chl = chlorite, Hbl = Hornblende, Pyx = Pyroxene, Bte = Biotite)

Table 4 Representative compositions of major minerals from the Metavolcanic.

Mineral	Percentage	Characteristics
Quartz	20%	Crystals are deformed by strain on grain contacts resulting in vertical shortening of grain contacts. Have undulose extinction and also mostly have cracks. They appear to be ‘squashed’ or crushed into pieces and form within the interstitial spaces of almost all the minerals. Strain has caused the quartz crystal to deform into domains with slightly different extinction angles. The quartz lacks alteration and no inclusions were seen.
Plagioclase Feldspar	15%	The plagioclase occurs as more or less equant euhedral to subhedral tabular crystals. They are white or gray lath-shaped grains with subhedral rectangular shapes. Most show albite twinning with few patches of crosshatched twinning in the cores of crystals. The plagioclases are more altered than the alkali feldspar and slightly higher relief. They show alteration into sericite along cracks and edges
Alkali Feldspar	4%	Dark-pink colour of K-feldspar is dominant. Have generally equidimensional grains and distortions in the originally white and/or pink lath-shaped and seems some have been crushed.
Pyroxene	10%	Flat, flaky grains of muscovite are present in excess of Biotite in Sample 1 as to the reverse in Sample 2. The Muscovites are anhedral to subhedral crystals and are in contacts with quartz crystals.
Biotite	10%	The flat, flaky grains with dark brown colour and cleavage in one direction have cracks and some alteration into sericite.

Hornblende	15%	The hornblende crystals are usually prismatic and are irregular in outline, wrapping round the feldspar and quartz.
Chlorite	15%	Fine-grained, matted-looking varieties often show undulose extinction. Light green is most common shade. Micaceous cleavage, often matted or feltlike appearance.
Other Accessory	2%	Appears to be dark or opaque both under cross and plane polars. Opaque (believe to be Fe-bearing oxide - ilmenite or magnetite) are seen to form along grain boundaries cracks of the Biotite and hornblende.

This is a fine grained igneous rock that has suffered minimal deformation, but fresh with largely unaltered major minerals. It is a well crystalline rock that contains quite a few amount of mica. Most of the minerals observed have been partially altered or is altering (grain shape and composition). There are some sorts of chloritization seen in the Hornblende and Biotite and sericitization also occur in the feldspars especially the Plagioclase.

The rock has been moderately deformed and some grains have been welded into their neighbours or penetrating them slightly. Alignment of micaceous minerals in a particular orientation may probably be as a result of small degree of deformation.

4.1.4 Quartzites

In hand specimen, the rock is grey to white in colour on freshly opened surfaces. They are hard and glassy and are sometimes difficult to distinguish from vein quartz. This probably resulted from the recrystallization of quartz grains. The minerals present in the rock are mainly quartz are

sometimes stained with iron. This colour is due to the abundance of felsic minerals which is basically quartz.

The rock is medium crystalline to coarse grained, hard, highly compact and weathered to some extent. On the weathered surfaces the colour changes from grey to pink due to stains of iron-oxides. Some samples have spotted brown surfaces. The rocks are very well indurated and less porous.



Fig. 4.11 Photograph of well indurated quartzite at South of Obuem. Photograph taken facing the North

Table 5 Representative compositions of major minerals from the Quartzite.

MINERAL	VOLUME (in %)	CHARACTERISTIC FEATURES
<p>Quartz</p> <p>Monocrystalline</p> <p>Polycrystalline</p>	<p>80%</p> <p>15%</p>	<p>Medium grained subhedral crystals with fractures and few fluid inclusions. The quartz lacks alteration and is crushed into pieces at some sections.</p> <p>Medium grained with wavy elongated boundaries that are commonly irregularly sutured.</p>
Sericite	3%	Clayey matrix cemented by a fine rock dust. Matrix is end products of broken and altered framework grains.
Accessory mineral	2%	Alteration product from the feldspars and lithic fragments appears to be chlorite and/or mica.

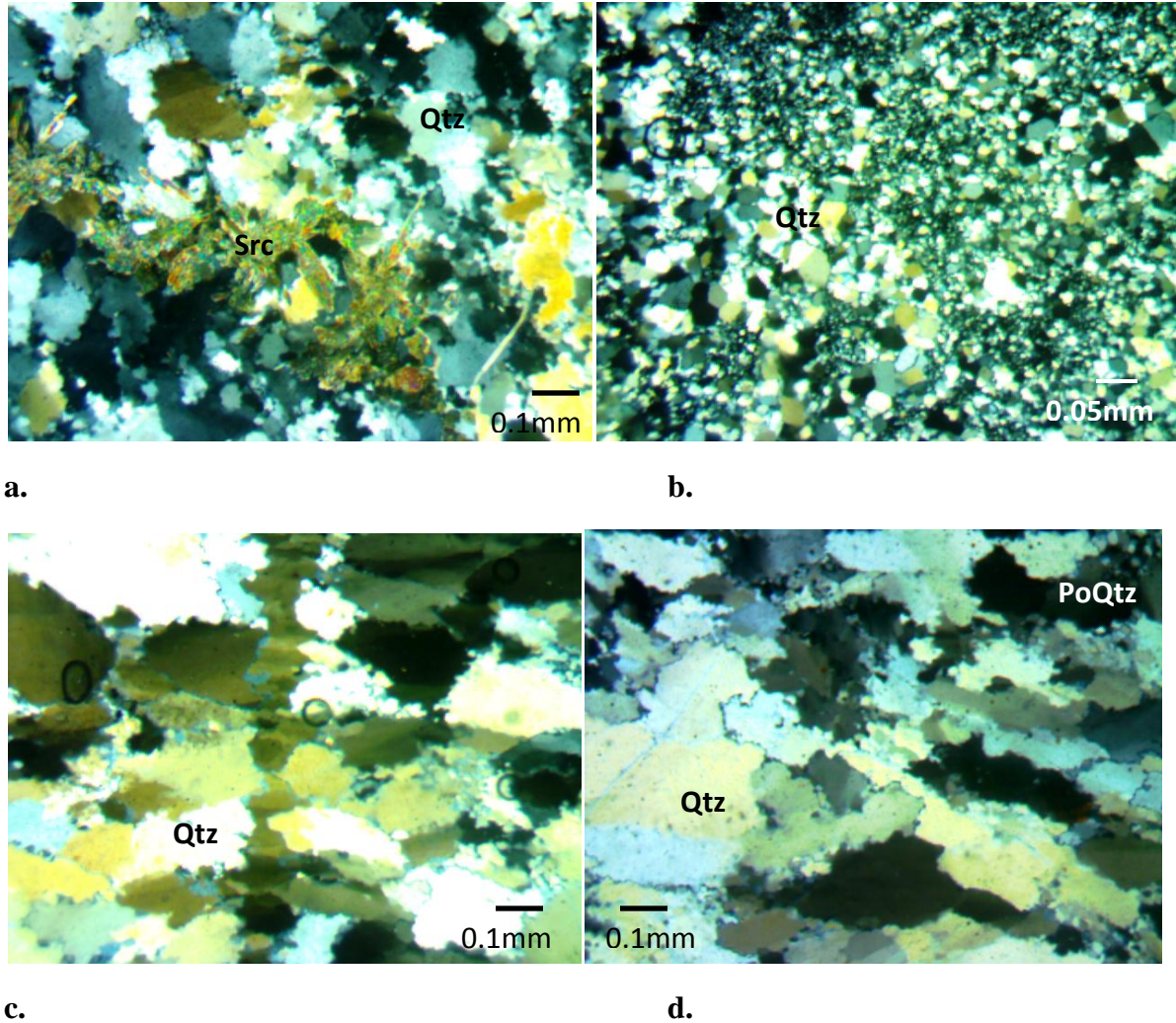


Fig.4.12 Photomicrograph of a Quartzite both in Crossed nicols.

(Mineral symbols: PoQtz = Polycrystalline quartz, Qtz = Quartz, Grndms = Src= Sericite)

Table 5 shows the representative compositions of major minerals within the Quartzite. As seen in figure 4.11, the rock showed a mosaic pattern with no preferred orientation of grains under thin section. Grains to grain boundaries are not well formed indicating metamorphic or deformational effects on the rock, that is, the rock had sutured boundaries. The quartz grains show undulose extinction with an interlocking texture which further gives evidence of the deformation of the rock with increase in temperature and pressure.

Thin section slides show well-aligned, strained and elongated closely packed quartz grains which are rounded to sub-rounded (Fig 4.11). There was replacement of parts of the matrix with sericite. This probably results from the alteration of feldspar, since feldspar has long been regarded as sensitive to climatic variability. Therefore no feldspars and rock fragments present.

4.2 STRUCTURAL MAPPING

Evidence from rocks studied in the area indicates several regimes of tectonic and metamorphic events. The various structures identified and mapped are discussed in the following section

4.2.1. Joints

The rock in the study area show parallel jointing. Joints are structural discontinuities that results from brittle deformational behaviour of rock. The jointing is more pronounced in the schist found at eastern part of the area than in the western parts (Fig.4.12). Two sets of joints are present in the area. These joints have various orientations but tend to follow two major trends at nearly right angles. The joint usually cut across foliation and hence deduced to be younger.



Fig.4.13 Photograph of schist that are thickly foliated and widely jointed outcropping half way between Kokotro and Obuem. Photo taken facing the north.

The rocks in the area generally have a NW/SE strike, have two general directions of dip which are opposite with most in a NE and SW direction (Fig.4.12). Joints in these outcrops have their strike parallel to the general strike of the area.

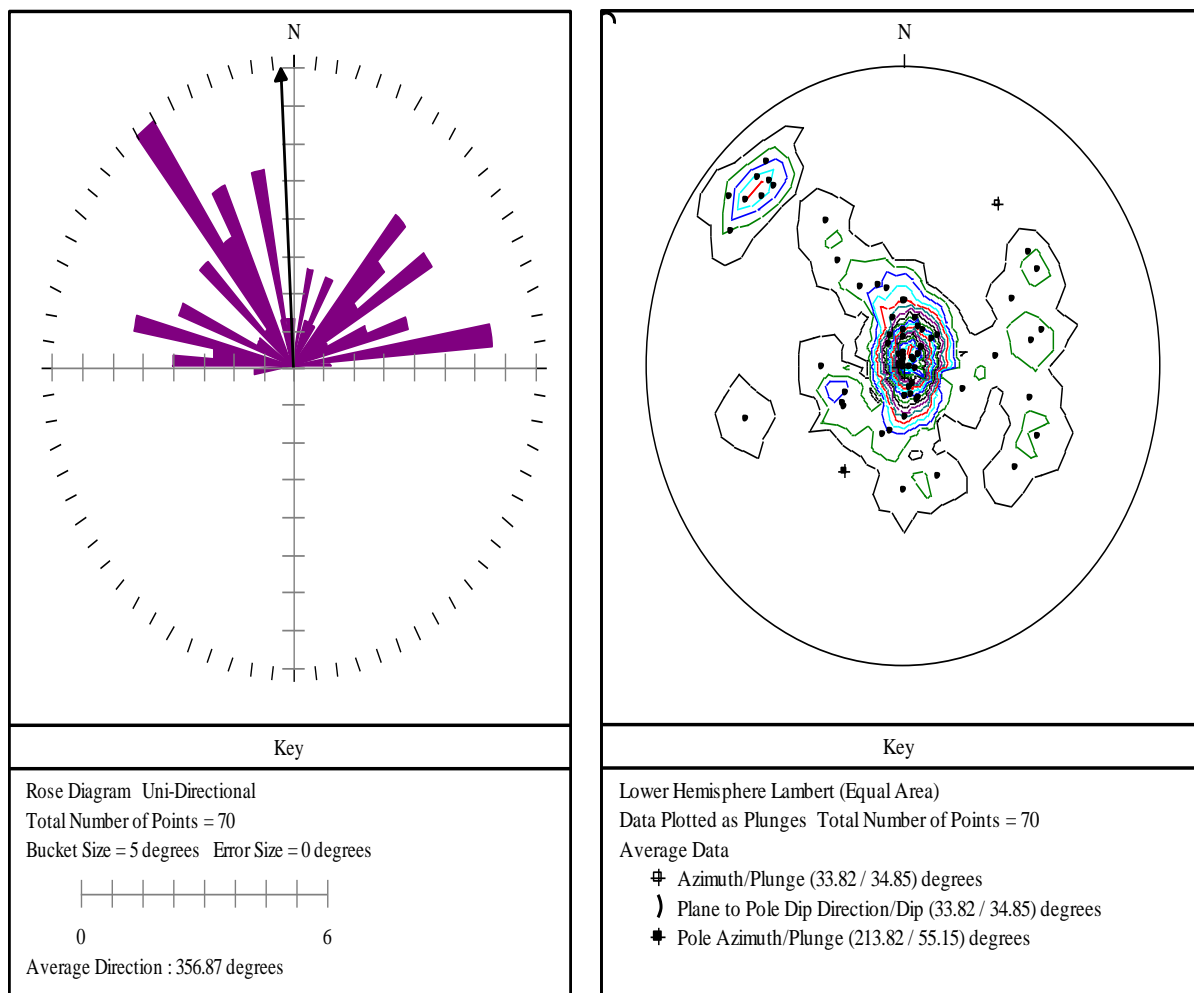


Fig.4.14 Stereographic projection of (a) Rose diagram showing a general NW-SE strike of joints (b) Plot to poles of joints within the lithologies

4.2.2. Folding

Folds are bending in strata that develop when layers of rock deform plastically. The rocks in the study area have few small scale folds. Most of these folds are along road cuts exposed because of erosion or have been truncated by various super-gene processes.

Most of these folds are truncated and are found in Twum area towards the central western boundary of the area. Here dip directions of the foliation surface measure changed direction from northwest to southeast in a rhythmic manner(Fig.4.14).

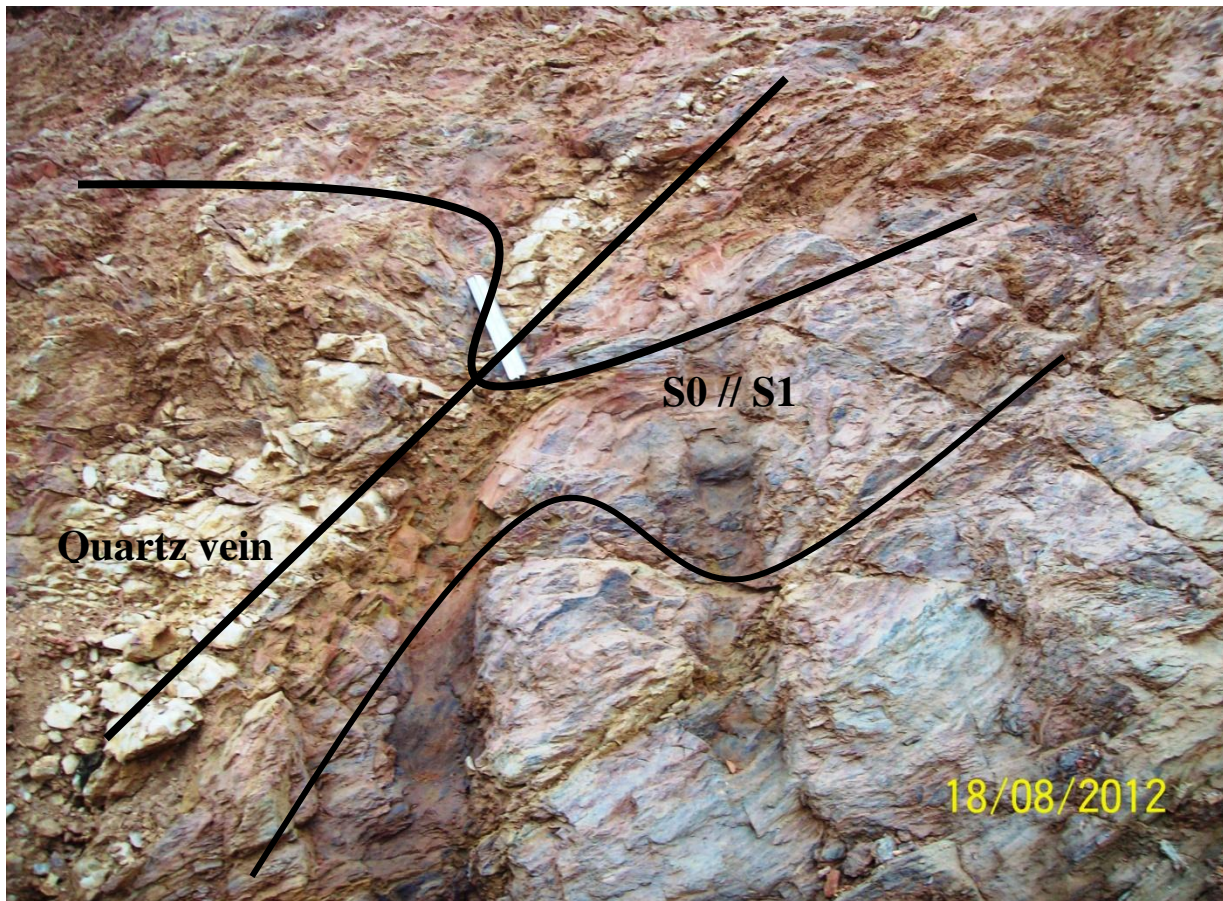


Fig.4.15 Photograph showing an initial asymmetric folding S0 axis and fold outcropping at East of Obuem. Photograph taken facing North

The anticline had a trend of 020 NNE and plunge of 80° ENE (Fig.4.15). This anticline has a width of 3.0 cm. The amplitude of the fold is 2m.

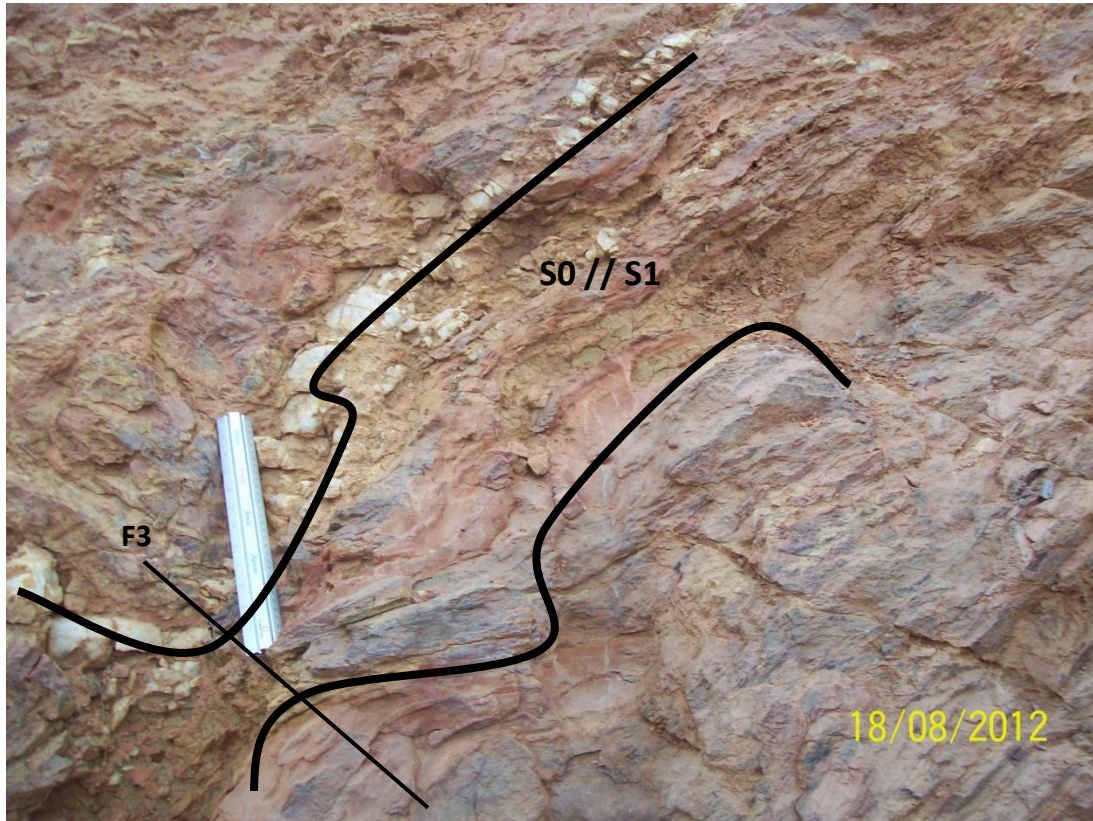


Fig.4.16 Photograph showing (a) truncated fold axis and anticlinal asymmetric fold outcropping at East of Obuem. Photo taken facing north

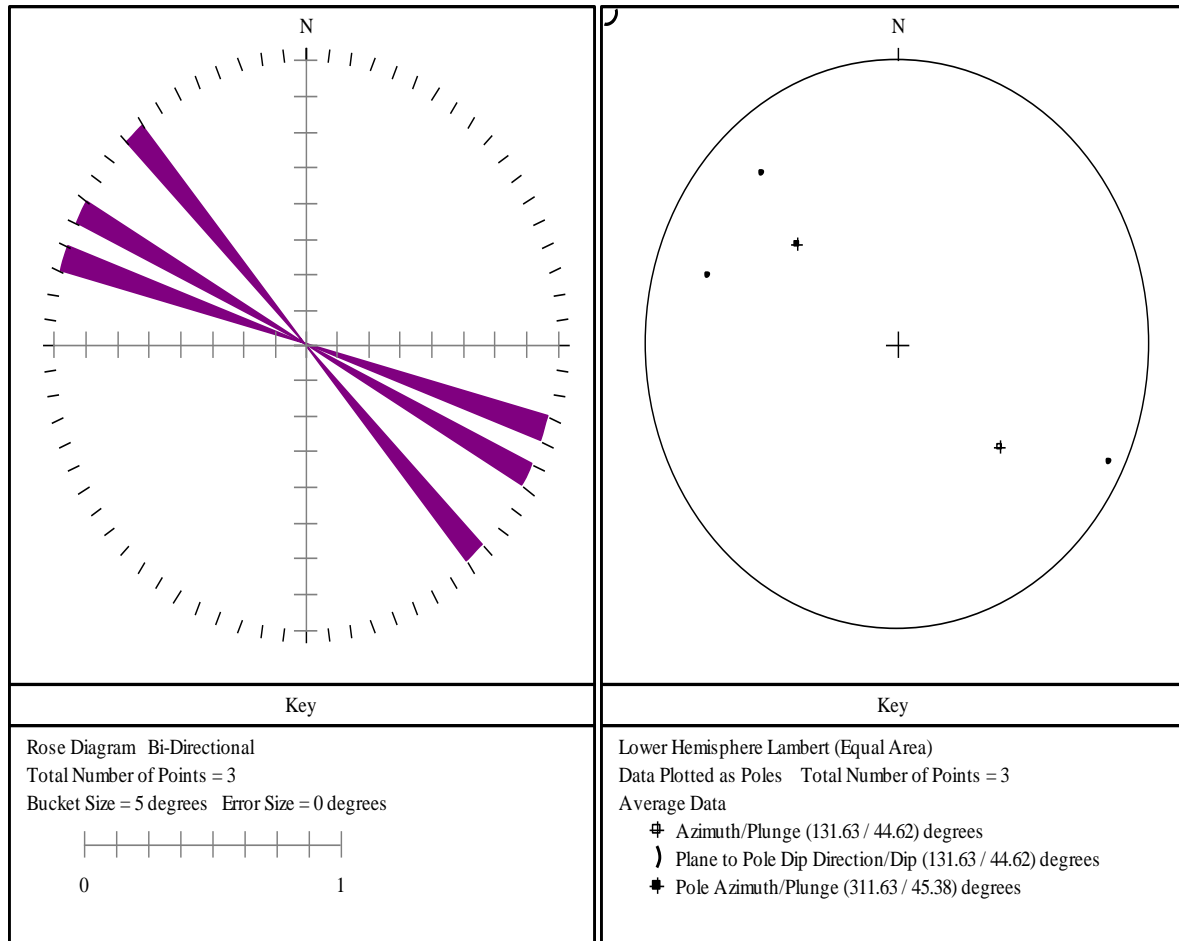


Fig.4.17 Stereographic projections of (a) plot of centroid of folds in rocks showing a north western – south eastern strike, and (b) rose diagram of folds

4.2.3. Lineation

The quartz veins have been squeezed out of the rock formation possibly due to compressive stress of the overlying rocks or differential weathering (Fig.4.17). Thickness of the veins range from 0.2cm to 0.5cm and stretches over 20cm to about 56cm in length. These quartz veins have a general 004⁰ trend.

The presence of the quartz veins is an indication of the deformation the area has undergone since quartz veins can only form by the solid state remobilization of silica (Raymond, 1995). They are thus sure indication that the area has experienced some level of tectonic activity and also indicate that there has been a minute amount metamorphism occurring.



Fig.4.18 Photograph of a Quartz vein leading from entrance into a mining pit. They are highly recrystallized.

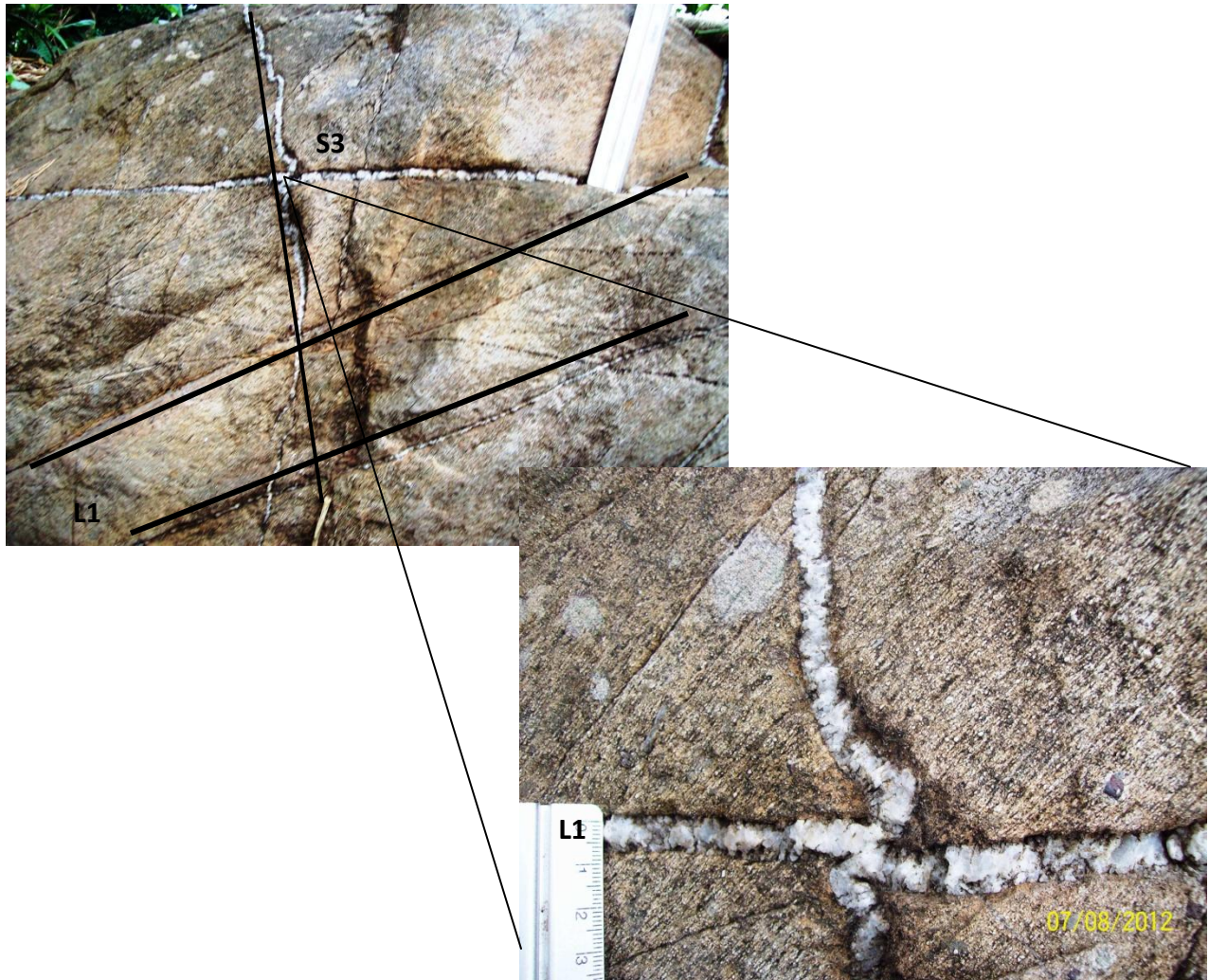


Fig. 4.19 Photograph showing concordant and discordant Quartz veins in schist rock. Good cross cutting relationship between S3 and So/S1

The quartz vein in Fig 4.17 probably served as a leading trace for the miners of old.

The veins are usually seen on foliation surfaces and result from host rocks due to deformational stresses and consequently mobilization and recrystallization of quartz to fill the already existing fractures (Raymond, 1995). The schists are thickly foliated and some are veined by quartz, which

are seen to be both concordant and discordant to the foliated surfaces (Fig.4.18). Quartz veining is very common. The veins observed are highly recrystallized.

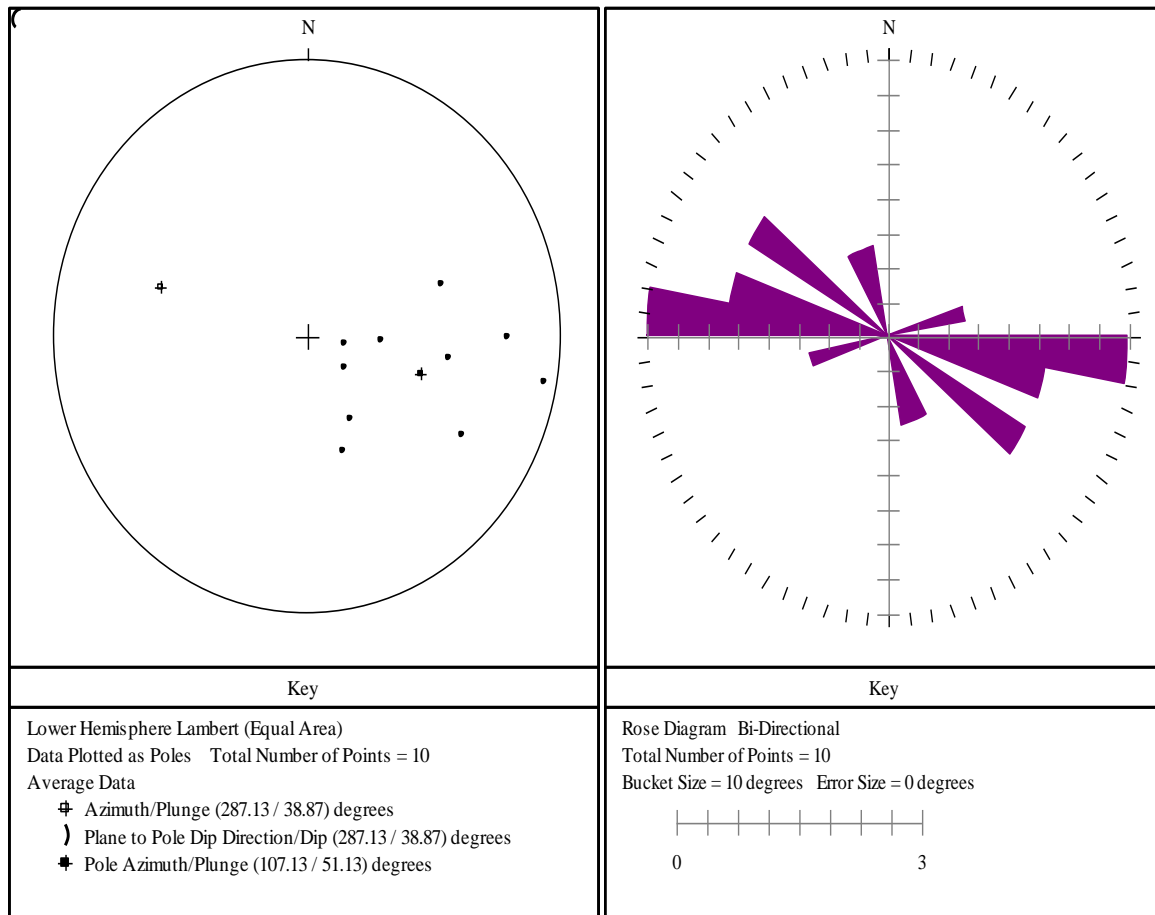


Fig.4.20 Stereographic projections of (a) plot of centroid of Quartz veins in rocks showing a west – north western strike, and (b) rose diagram of Quartz veins

4.2.4. Foliations

Foliation is the property of rocks to break along approximately parallel surfaces (Billings, 2006) due to the alignment of flakes of micas and elongate quartz crystals. Ductile deformation which resulted in the formation of foliation leads to permanent shape changes throughout the rock masses. The quartz crystals are elongated, strain and has preferred alignment which is evidence of foliation.

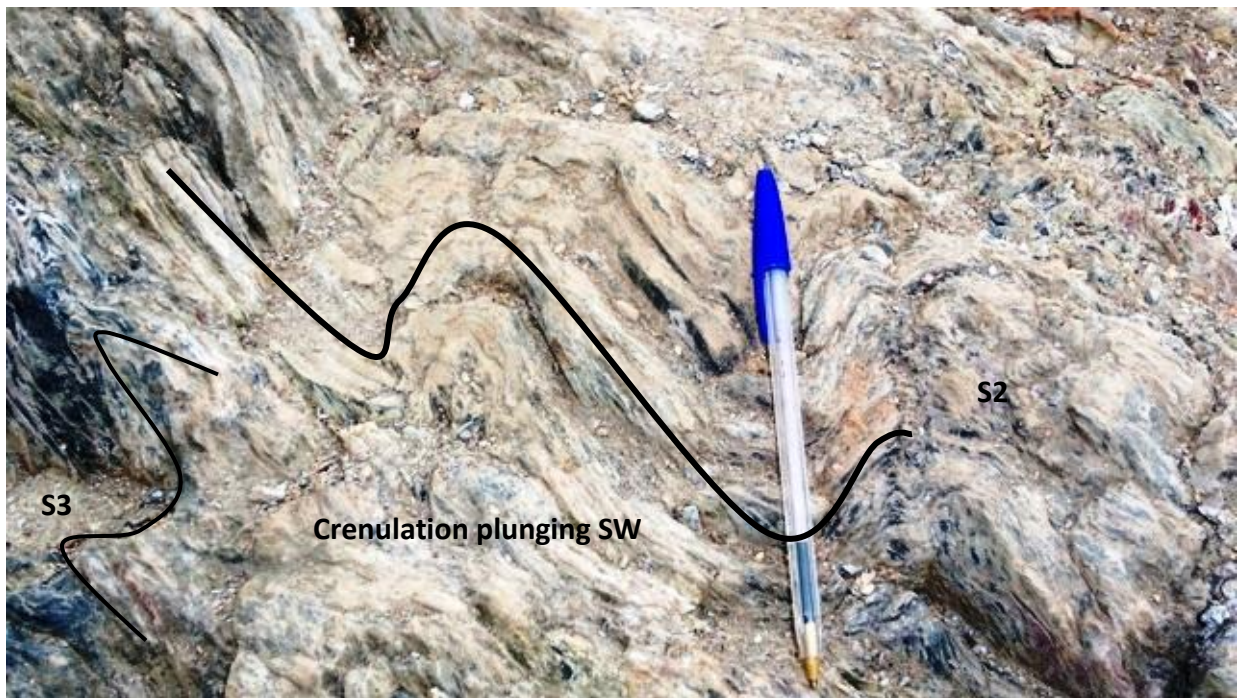


Fig.4.21 Photograph of foliations observed in Metavolcanic. Photo taken facing North.

The foliations were observed in both the metavolcanics (Fig.4.20) and the metasediments (Fig.4.22). The foliations formed as a result of ductile responses to incident stress causing realignment of minerals in the direction of least stress. It can be inferred that the forces that caused the deformation were from NW-SE and NE-SW.



Fig.4.22 Photograph of crenulations observed in Greywacke.



Fig.4.23 Photograph of thickly foliated Graphitic Phyllites. Photo taken facing west

4.3 GEOCHEMISTRY

4.3.1. Composition of rock groupings

The major, minor, trace and REE elements of 25 samples were geochemically analyzed as shown in the Table below. Thirteen (13) major elements (SiO₂, Al₂O₃, total Fe as Fe₂O₃, CaO, MgO, Na₂O, K₂O, P₂O₅, SrO, MnO, TiO₂, MnO, P₂O₅, SrO, and BaO) and 31 minor and trace elements (Nb, Zr, Y, Sr, Rb, Sc, V, Cr, Ni, Cu, Zn, Ba, La, Ce, Pr, Nd, Eu, Sm, Gd, Tb, Dy, Ho, Er, Li, Yb, Lu, Hf, Ta, Pb, Th, and U) were selected for analysis in this study.

From the geochemical result it could be deduced that the metavolcanic rocks (STOB20F1, STKT20, KTR02A9, OBST02A2) have low silica (SiO₂) content ranging from 45 to 50wt% whilst Fe₂O₃ +MgO range from 4 to 8wt%. Al₂O₃ values range from 0.33 to 0.34 wt %. That of K₂O+Na₂ is from 4 to 8wt% and the values of CaO range from 2 to 3 wt%. Total iron (Fe₂O₃t) range between 8-18.56 wt% and MgO values are between 1 and 3 wt%.

Table 6: Major elements of rock samples from the Obuem concession Ash Reg., Ghana.

Samples	SiO ₂	Al ₂ O ₃	Fe ₂ O ₃	CaO	MgO	Na ₂ O	K ₂ O	Cr ₂ O ₃	TiO ₂	MnO	P ₂ O ₅	SrO	BaO	LOI	Total
	%	%	%	%	%	%	%	%	%	%	%	%	%	%	%
OBST02A2	47.56	12.35	6.28	8.17	6.79	2.03	0.82	0.08	0.48	0.12	0.109	0.05	0.01	14.55	99.39
OBST02A6	55.81	15.25	5.93	4.76	3.15	2.21	1.86	0.02	0.47	0.13	0.113	0.04	0.05	9.55	99.33
OBST03A4	51.55	17.35	8.61	4.6	3.88	3.47	1.33	0.02	0.65	0.11	0.154	0.04	0.03	7.13	98.94
OBST07A3	53.33	16.85	6.04	4.67	3.36	4.59	1.28	0.01	0.52	0.09	0.118	0.08	0.05	8.62	99.61
OBST08A7	98.19	0.58	0.31	0.07	0.15	0.06	0.04	0.009	0.009	0.009	0.012	0.009	0.009	0.25	99.65
OBST10A4	51.62	15.85	7.31	5.16	3.91	3.34	0.93	0.05	0.7	0.11	0.237	0.06	0.03	8.82	98.12
OBST11A5	52.18	12.5	8.36	4.93	6.82	2.35	0.86	0.1	0.72	0.1	0.237	0.03	0.02	9.71	98.93
KTR01A8	98.6	0.23	0.28	0.04	0.1	0.03	0.02	0.009	0.009	0.009	0.013	0.009	0.009	0.63	99.93
KTR02A9	49.23	9.75	9.47	9.77	14.49	1.22	0.86	0.18	0.24	0.17	0.142	0.02	0.02	3.88	99.44
KTR03A11	63.66	15.56	5.87	3.6	2.32	3.47	1.65	0.01	0.64	0.07	0.165	0.05	0.08	2.25	99.41
STKT04	64.23	15.36	5.79	3.62	2.33	3.43	1.62	0.02	0.63	0.07	0.163	0.05	0.08	2.16	99.55
STKT10	57.81	13.94	7.66	5.47	6.44	2.32	1.34	0.08	0.64	0.12	0.23	0.06	0.07	2.88	99.05
STKT20	48.78	9.4	9.67	10.09	14.76	1.2	0.62	0.19	0.23	0.18	0.134	0.02	0.01	4.03	99.31
STKT30	62.88	15.66	5.97	3.63	2.37	3.39	1.72	0.02	0.65	0.07	0.177	0.05	0.08	2.33	99
STOB07C	53.02	16.88	6.1	4.68	3.48	4.33	1.25	0.01	0.52	0.09	0.115	0.09	0.04	8.63	99.24
STOB08G	98.52	0.33	0.38	0.03	0.11	0.04	0.02	0.009	0.009	0.009	0.012	0.009	0.009	0.1	99.51
STOB10B	55.62	15.98	6.44	4.23	3.14	2.13	1.95	0.02	0.53	0.12	0.123	0.04	0.05	8.64	99.02
STOB10D	51.16	16.8	7.26	4.76	3.94	3.38	0.97	0.05	0.75	0.1	0.247	0.07	0.02	8.92	98.43
STOB11E	51.33	12.43	8.47	5.34	7.14	2.15	0.94	0.1	0.71	0.11	0.244	0.03	0.03	10.35	99.37
STOB20F1	47.43	12.09	6.4	8.35	6.66	2.04	0.82	0.08	0.48	0.13	0.11	0.05	0.02	14.45	99.1

STOB20F2	53.81	17.16	8.21	4.06	3.69	3.48	1.39	0.01	0.62	0.1	0.146	0.04	0.03	6.24	99
BRFST01A8	67.33	15.59	2.88	3.05	1.44	4.58	2.72	0.01	0.44	0.04	0.173	0.11	0.14	0.59	99.09
STBF010A	67.61	15.68	2.78	2.86	1.37	4.53	2.84	0.009	0.41	0.04	0.165	0.11	0.14	0.51	99.06
KONST04	91.03	3.08	0.67	0.02	0.18	0.07	0.66	0.02	0.1	0.009	0.017	0.009	0.03	3.97	99.86
KONST05	98.64	0.14	0.52	0.01	0.07	0.02	0.01	0.009	0.009	0.01	0.013	0.009	0.009	0.38	99.76

Table 6. REEs of rock samples from the Obuem concession Ash Reg., Ghana

Analyte	Gd	Ho	Lu	Nd	Pr	Sm	Tb	Tm	Yb
	ppm	ppm	Ppm	ppm	ppm	ppm	ppm	ppm	ppm
OBST02A2	1.54	0.17	0.13	10	2.41	2.11	0.19	0.09	0.69
OBST02A6	1.58	0.19	0.14	7.9	1.85	1.84	0.21	0.09	0.69
OBST03A4	1.43	0.16	0.11	8	1.85	1.78	0.17	0.08	0.6
OBST07A3	<0.05	0.01	0.009	0.3	0.06	0.06	0.01	0.009	<0.03
OBST08A7	4.14	0.45	0.22	26.4	6.57	5.24	0.5	0.2	1.28
OBST10A4	3.46	0.34	0.19	21.9	5.18	4.59	0.4	0.15	1.04
OBST11A5	0.09	0.02	0.01	0.5	0.14	0.1	0.02	0.01	0.05
KTR01A8	1.28	0.25	0.12	4.6	1.03	1.12	0.19	0.11	0.71
KTR02A9	3.94	0.66	0.26	23.3	6.04	4.52	0.57	0.28	1.64
KTR03A11	4.03	0.66	0.26	23.7	6.18	4.52	0.58	0.28	1.63
STKT04	4.98	0.66	0.23	28.6	7.04	5.78	0.66	0.25	1.47
STKT10	1.29	0.26	0.12	4.6	1.03	1.08	0.2	0.12	0.73
STKT20	3.96	0.66	0.27	22.9	5.93	4.45	0.56	0.28	1.67
STKT30	1.39	0.16	0.12	7.9	1.86	1.74	0.17	0.08	0.59
STOB07C	<0.05	0.01	0.009	0.2	0.06	0.04	0.009	0.009	<0.03
STOB08G	1.81	0.2	0.16	10.6	2.59	2.22	0.22	0.11	0.8
STOB10B	4.14	0.45	0.22	26.1	6.46	5.27	0.5	0.2	1.28
STOB10D	3.59	0.35	0.2	22.7	5.41	4.78	0.41	0.16	1.05
STOB11E	1.93	0.22	0.13	10.6	2.59	2.22	0.24	0.11	0.75
STOB20F1	1.53	0.18	0.13	7.1	1.68	1.66	0.19	0.09	0.68
STOB20F2	3.79	0.27	0.12	34.8	9.22	5.86	0.39	0.1	0.6
BRFST01A8	3.85	0.27	0.12	33.2	8.81	5.81	0.4	0.09	0.59
STBF010A	0.58	0.16	0.11	3.3	0.88	0.71	0.11	0.09	0.63
KONST04	0.06	0.01	0.009	0.6	0.16	0.09	0.01	0.009	0.03

Table 7. Trace elements of rock samples from the Obuem concession Ash Reg., Ghana.

Sample	Ba	Ce	Cr	Cu	Hf	In	La	Li	Nb	Ni	Pb	Rb	Sc	Sr	Ta	Th	U	V	Y	Zn	Zr
OBST02A2	200	19.35	364	50.7	1.9	0.041	8.4	59	2.3	110.5	4.6	29.6	24	546	0.16	1.3	0.5	129	6	65	73.1
OBST02A6	450	19.3	89	46.9	2	0.046	8	35.7	2.6	37.4	3.7	36.8	15.6	450	0.17	1.3	0.5	126	4.2	67	73.5
OBST03A4	340	14.45	91	47.4	1.7	0.047	6	57.3	1.3	36.8	3.4	19.7	21.4	429	0.08	0.8	0.4	184	4.3	94	61.3
OBST07A3	460	14.1	60	27	1.8	0.043	5.8	33.3	1.9	33.8	3.4	17.5	13.7	832	0.12	0.9	0.4	117	3.7	75	63
OBST08A7	10	0.5	16	3.3	0.09	0.0049	0.49	1.1	0.09	1.6	0.49	1.9	0.9	11.5	0.049	0.19	0.09	6	0.2	3	1.4
OBST10A4	320	53.4	273	40.4	3.7	0.049	23.9	56.1	3.7	83.9	7.1	21.3	19.3	683	0.23	3.5	1	151	12.1	73	141
OBST11A5	320	40.1	489	40	2.7	0.046	17.5	38.4	1.1	187.5	4.2	20.2	26.2	319	0.07	2.2	0.7	166	9	83	104
KTR01A8	10	1.38	24	2.3	0.1	0.0049	0.8	0.8	0.2	2.7	1	0.8	0.4	8.1	0.049	0.19	0.2	2	0.6	3	6.9
KTR02A9	220	7.37	790	130	0.4	0.036	3.8	32.2	0.8	301	2.7	24.9	42.3	240	0.049	0.5	0.2	163	7.1	59	12.5
KTR03A11	740	50.8	72	45.5	2.6	0.045	23.5	39.3	6.3	30.9	14.2	46.7	13.7	504	0.46	5.3	1.7	110	18.5	77	97.4
STKT04	720	51.8	74	37.3	2.6	0.044	25	37.6	5.8	30.7	9.1	45.7	13.4	488	0.44	4.7	1.6	107	18.7	75	93.6
STKT10	700	56.9	402	31.5	2.4	0.046	26.2	38.1	6.4	138.5	7	27.7	19.6	646	0.39	3.4	1.1	142	18	71	97.8
STKT20	160	7.48	842	48.9	0.4	0.032	3.7	32.5	0.8	299	2.2	18.4	43.8	243	0.05	0.5	0.2	159	7	63	12.6
STKT30	760	50	81	41.2	2.7	0.043	23.3	39.2	6	30.7	8.3	45	13.5	497	0.44	4.6	1.6	112	18.5	74	98.1
STOB07C	450	14.45	67	29.1	1.8	0.04	6	33.4	1.9	36	3.4	17.9	14.1	874	0.12	1	0.4	118	3.7	74	65.6
STOB08G	10	0.44	22	2.6	0.09	0.0049	0.49	0.6	0.1	2.1	0.49	1	0.4	7.9	0.049	0.19	0.09	3	0.1	2	1.1
STOB10B	500	20.7	118	61.9	2.5	0.049	8.6	40.7	2.9	49.1	4.5	41.5	18.1	476	0.2	1.6	0.6	143	4.5	79	86.6
STOB10D	340	52	297	46.9	4	0.05	22.6	61.4	4	87.2	6.5	17.5	19.6	719	0.25	3.3	1	167	11.8	83	151.5
STOB11E	330	42.4	500	40.6	2.7	0.048	18.7	37.6	1.1	189.5	4.7	27.2	27.7	341	0.07	2.3	0.7	172	9.3	82	104.5
STOB20F1	200	20.9	366	36.6	1.9	0.037	9.1	53.5	2.3	121.5	4	28.4	23	533	0.15	1.4	0.5	127	5.8	61	72.8
STOB20F2	350	12.85	84	51.6	1.7	0.042	5.5	49.6	1.2	36.1	3.5	26.1	22.1	404	0.08	0.8	0.4	183	4	87	58.9
BRFST01A8	0 117 127	76.2	33	6.8	4.2	0.043	36.7	48.1	4.2	19.9	16.5	73.5	6.4	1020	0.27	7	1.9	39	7.4	72	159.5
STBF010A	0	78.6	30	3.6	4.1	0.042	34.1	47.5	4.2	19.4	16.6	86.4	6.2	1020	0.25	6.7	1.8	38	7.5	70	161.5
KONST04	360	9.75	166	24.8	0.8	0.015	4	4.1	0.9	3.7	2.5	24.8	4	22.5	0.06	1	1.3	158	4.5	4	47.2
KONST05	10	1.45	17	1.7	0.1	0.0049	0.8	0.5	0.1	1.4	0.6	0.9	0.2	5.8	0.049	0.2	0.2	2	0.3	1.9	4.1

4.3.2. Classification of Metavolcanic rocks

The metavolcanics show SiO₂ content ranging from 47 to 49wt% and Al₂O₃ is 12-17wt%. The Fe₂O₃ content ranges from 1-8wt%, TiO₂ is 0.4-0.7wt% and MnO is 0.09-0.18wt%. CaO ranges from 4-8wt% and that may indicate high secondary alteration. Furthermore the high value of LOI >8 indicate that the primary mineral assemblage has been severely altered. Pearce and Cann (1973) indicated that the low TiO₂ contents of this rock resemble those of igneous rocks from depleted are basalt.

The classification scheme proposed by Middlemost (1975) is used and majority of the metavolcanic samples are found in the region of the sub-alkalic rocks. This indicates the sub-alkalic affinity of the rocks is of Tholeiitic nature.

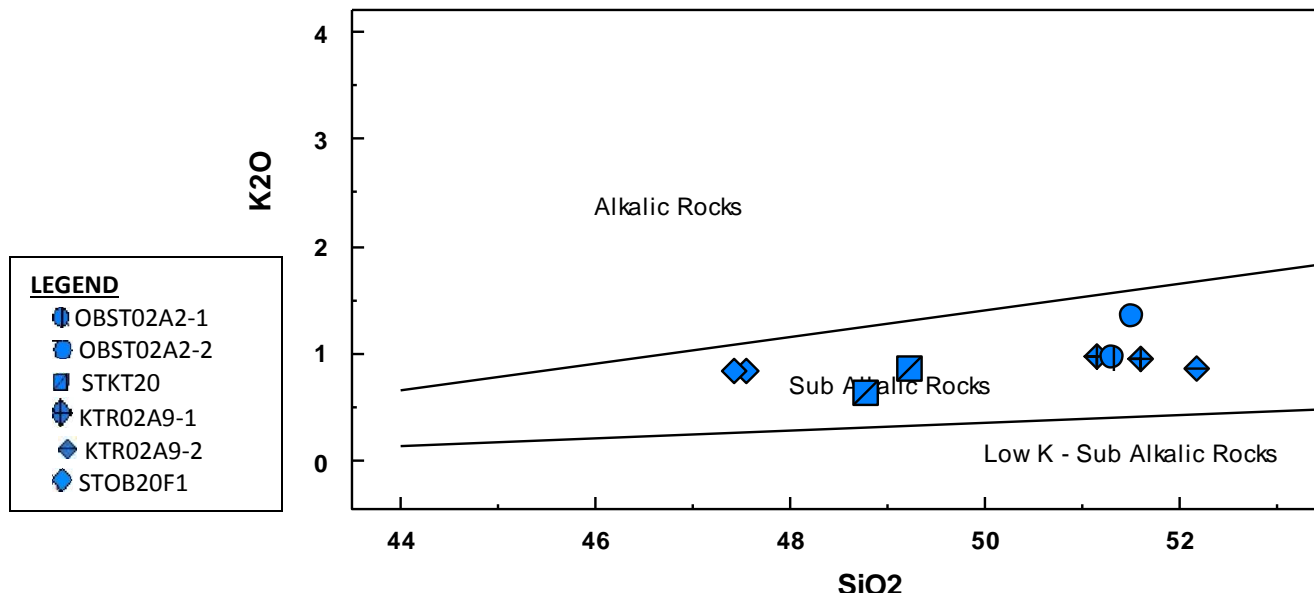


Fig. 4.24 TAS Alkalis-Silica Classification of Obuem Mine metavolcanics on a Na₂O+K₂O – SiO₂ diagram (after Middlemost 1975).

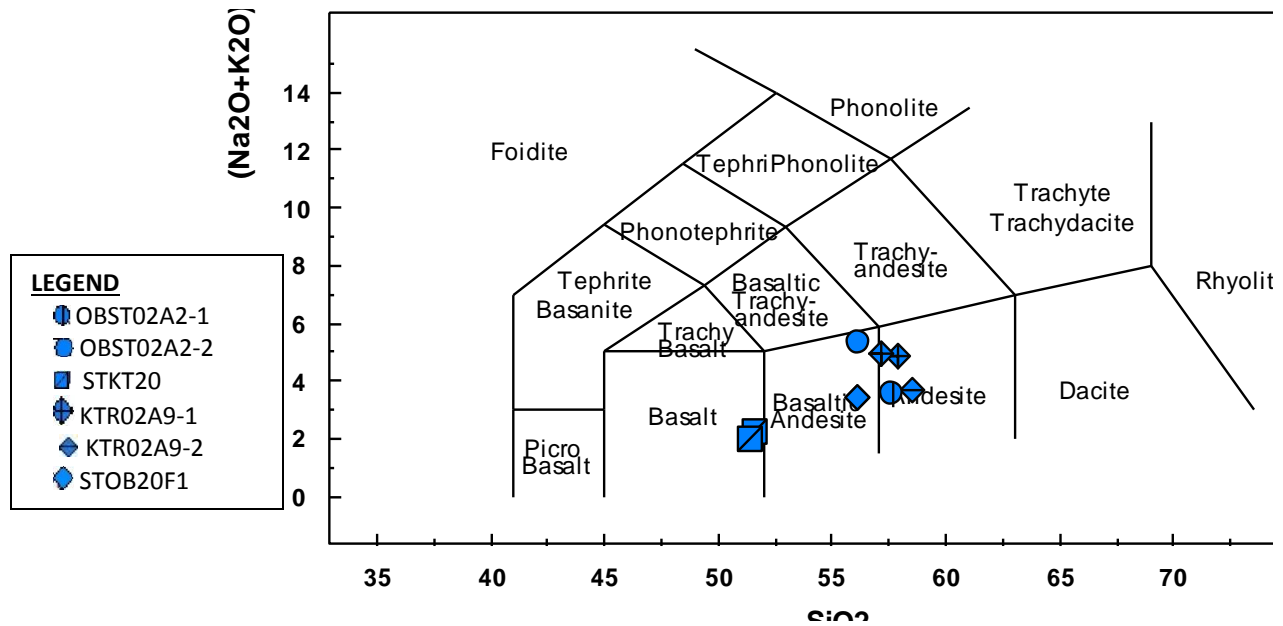


Fig. 4.25 TAS Alkalis-Silica Classification of Obuem Mine metavolcanics on a Na₂O+K₂O – SiO₂ diagram after LeBas et al., 1986

The AFM diagram depicts the metavolcanic rock samples to be of calc-alkaline nature.

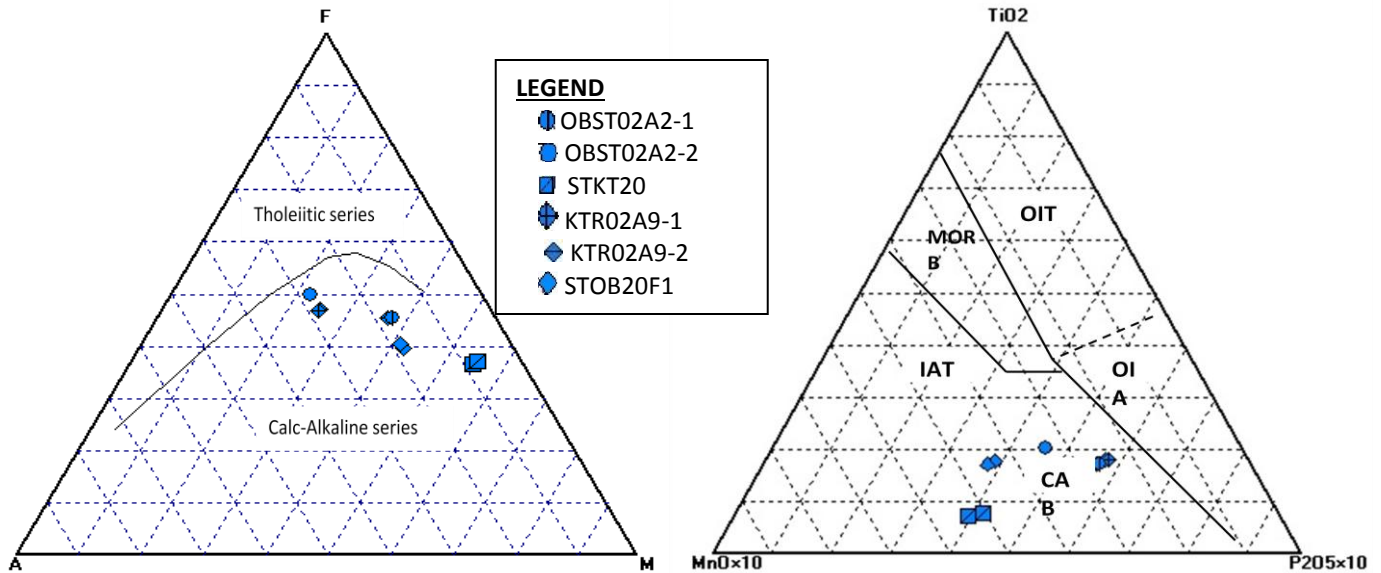


Fig 4.26a. AFM Triangular Plot showing calc-alkaline and tholeiitic boundary fields from the Obuem samples. (After Sun & McDonough (1989))

Fig 4.26b. The MnO-TiO₂-P₂O₅ discrimination diagram for basalts and basaltic andesites (after Mullen,1983). The fields are MORB, OIT – ocean island tholeiite, OIA – ocean island alkali, CAB – island arc Calc-alkaline basalt, IAT – island arc tholeiite.

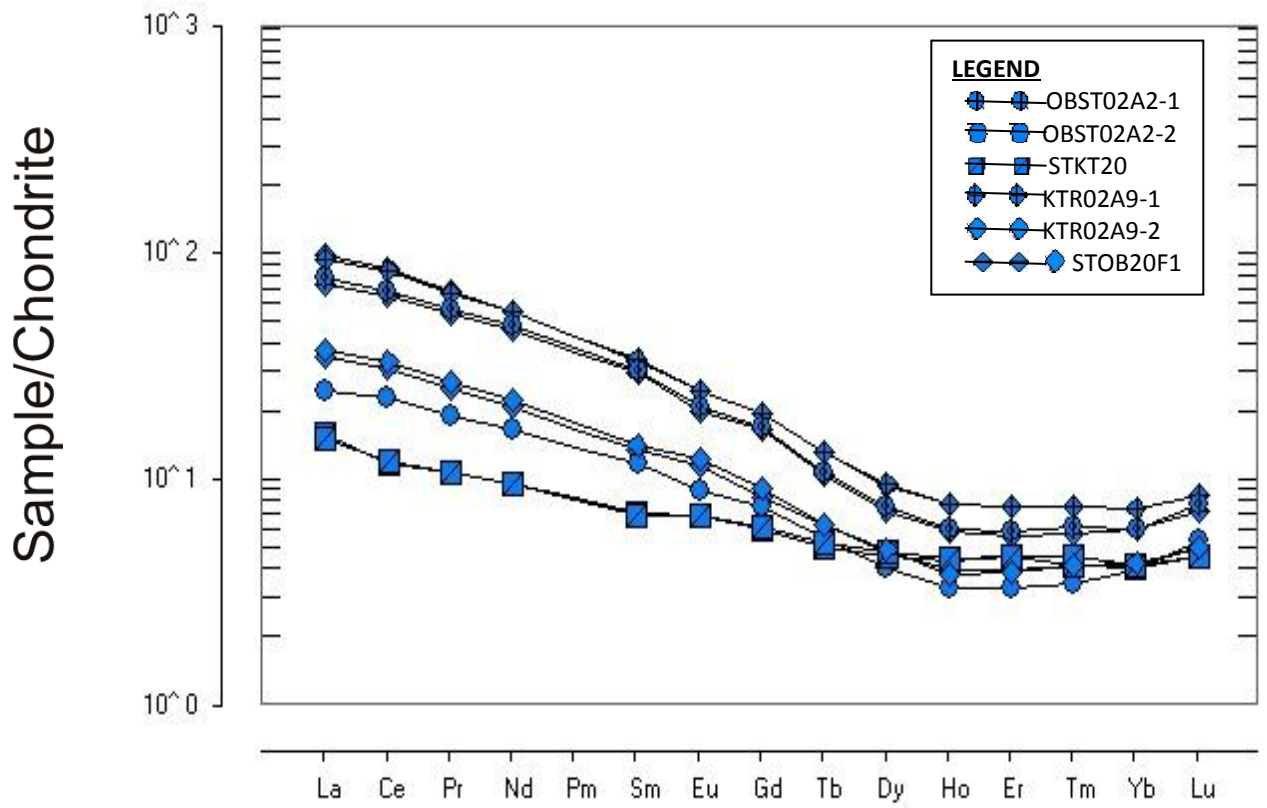


Fig. 4.27 Spider plots for the REE normalized against the Chondrite after Sun & McDonough (1989).

Table 8: Major elements of Mafic rock samples from the Obuem concession Ash Reg., Ghana.

Sample	SiO ₂	TiO ₂	Al ₂ O ₃	Fe ₂ O ₃	Na ₂ O	MgO	K ₂ O	Cr ₂ O ₃	CaO	MnO	P ₂ O ₅	SrO	BaO	LOI	Total
OBST02A2	47.56	0.48	12.35	6.28	2.03	6.79	0.82	0.08	8.17	0.12	0.109	0.05	0.01	14.55	99.39
KTR02A9	49.23	0.24	9.75	9.47	1.22	14.49	0.86	0.18	9.77	0.17	0.142	0.02	0.02	3.88	99.44
STKT20	48.78	0.23	9.4	9.67	1.2	14.76	0.62	0.19	10.09		0.134	0.02	0.01	4.03	99.31
STOB20F1	47.43	0.48	12.09	6.4	2.04	6.66	0.82	0.08	8.35	0.13	0.11	0.05	0.02	14.45	99.1

Table 9: REEs elements of Mafic rock samples from the Obuem concession Ash Reg., Ghana.

SAMPLE	Dy	Er	Eu	Gd	Ho	Lu	Nd	Pr	Sm	Tb	Tm	Yb
	ppm	ppm	ppm	ppm	ppm	ppm	ppm	ppm	ppm	ppm	ppm	ppm
OBST02A2	1.23	0.67	0.68	1.76	0.23	0.13	9.9	2.42	2.12	0.24	0.11	0.73
KTR02A9	1.2	0.77	0.41	1.28	0.25	0.12	4.6	1.03	1.12	0.19	0.11	0.71
STKT20	1.23	0.78	0.41	1.29	0.26	0.12	4.6	1.03	1.08	0.2	0.12	0.73
STOB20F1	1.26	0.66	0.73	1.93	0.22	0.13	10.6	2.59	2.22	0.24	0.11	0.75

4.3.3. Geochemistry of Metasediments

Table 10: Major elements of Metasediments from the Obuem concession in the Ash Reg., Ghana

Sample	SiO ₂	TiO ₂	Al ₂ O ₃	Fe ₂ O ₃	Na ₂ O	MgO	K ₂ O	CaO	MnO	P ₂ O ₅	LOI	Total
OBST02A6	55.81	0.47	15.25	5.93	2.21	3.15	1.86	4.76	0.13	0.113	9.55	99.33
OBST03A4	51.55	0.65	17.35	8.61	3.47	3.88	1.33	4.6	0.11	0.154	7.13	98.94
OBST07A3	53.33	0.52	16.85	6.04	4.59	3.36	1.28	4.67	0.09	0.118	8.62	99.61
OBST10A4	51.62	0.7	15.85	7.31	3.34	3.91	0.93	5.16	0.11	0.237		98.12
OBST11A5	52.18	0.72	12.5	8.36	2.35	6.82	0.86	4.93	0.1	0.237	9.71	98.93
KTR03A11	63.66	0.64	15.56	5.87	3.47	2.32	1.65	3.6	0.07	0.165	2.25	99.41
STKT04D	64.23	0.63	15.36	5.79	3.43	2.33	1.62	3.62	0.07	0.163	2.16	99.55
STKT10	57.81	0.64	13.94	7.66	2.32	6.44	1.34	5.47	0.12	0.23	2.88	99.05
STKT30	62.88	0.65	15.66	5.97	3.39	2.37	1.72	3.63	0.07	0.177	2.33	99
STOB07C	53.02	0.52	16.88	6.1	4.33	3.48	1.25	4.68	0.09	0.115	8.63	99.24
STOB10B	55.62	0.53	15.98	6.44	2.13	3.14	1.95	4.23	0.12	0.123	8.64	99.02
STOB10D	51.16	0.75	16.8	7.26	3.38	3.94	0.97	4.76	0.1	0.247	8.92	98.43
STOB11E	51.33	0.71	12.43	8.47	2.15	7.14	0.94	5.34	0.11	0.244	10.35	99.37
STOB20F2	53.81	0.62	17.16	8.21	3.48	3.69	1.39	4.06	0.1	0.146	6.24	99
BRFST01A8	67.33	0.44	15.59	2.88	4.58	1.44	2.72	3.05	0.04	0.173	0.59	99.09
STBF010A	67.61	0.41	15.68	2.78	4.53	1.37	2.84	2.86	0.04	0.165	0.51	99.06

Table 11: REE of Metasediments from the Obuem concession in the Ash Reg., Ghana

SAMPLE	Dy ppm	Er ppm	Eu ppm	Gd ppm	Ho ppm	Lu ppm	Nd ppm	Pr ppm	Sm ppm	Tb ppm	Tm ppm	Yb ppm
OBST02A6	0.92	0.52	0.55	1.54	0.17	0.13	10	2.41	2.11	0.19	0.09	0.69
OBST03A4	1.06	0.56	0.53	1.58	0.19	0.14	7.9	1.85	1.84	0.21	0.09	0.69
OBST07A3	0.88	0.49	0.55	1.43	0.16	0.11	8	1.85	1.78	0.17	0.08	0.6
OBST10A4	2.45	1.27	1.45	4.14	0.45	0.22	26.4	6.57	5.24	0.5	0.2	1.28
OBST11A5	1.9	0.96	1.19	3.46	0.34	0.19	21.9	5.18	4.59	0.4	0.15	1.04
KTR03A11	3.27	1.87	1.17	3.94	0.66	0.26	23.3	6.04	4.52	0.57	0.28	1.64
STKT04	3.24	1.9	1.17	4.03	0.66	0.26	23.7	6.18	4.52	0.58	0.28	1.63
STKT10	3.49	1.8	1.49	4.98	0.66	0.23	28.6	7.04	5.78	0.66	0.25	1.47
STKT30	3.28	1.91	1.14	3.96	0.66	0.27	22.9	5.93	4.45	0.56	0.28	1.67
STOB07C	0.85	0.48	0.54	1.39	0.16	0.12	7.9	1.86	1.74	0.17	0.08	0.59
STOB10B	1.04	0.6	0.66	1.81	0.2	0.16	10.6	2.59	2.22	0.22	0.11	0.8
STOB10D	2.5	1.29	1.45	4.14	0.45	0.22	26.1	6.46	5.27	0.5	0.2	1.28
STOB11E	1.95	0.99	1.25	3.59	0.35	0.2	22.7	5.41	4.78	0.41	0.16	1.05
STOB20F2	0.98	0.54	0.54	1.53	0.18	0.13	7.1	1.68	1.66	0.19	0.09	0.68
BRFST01A8	1.69	0.66	1.6	3.79	0.27	0.12	34.8	9.22	5.86	0.39	0.1	0.6
STBF010A	1.69	0.66	1.63	3.85	0.27	0.12	33.2	8.81	5.81	0.4	0.09	0.59

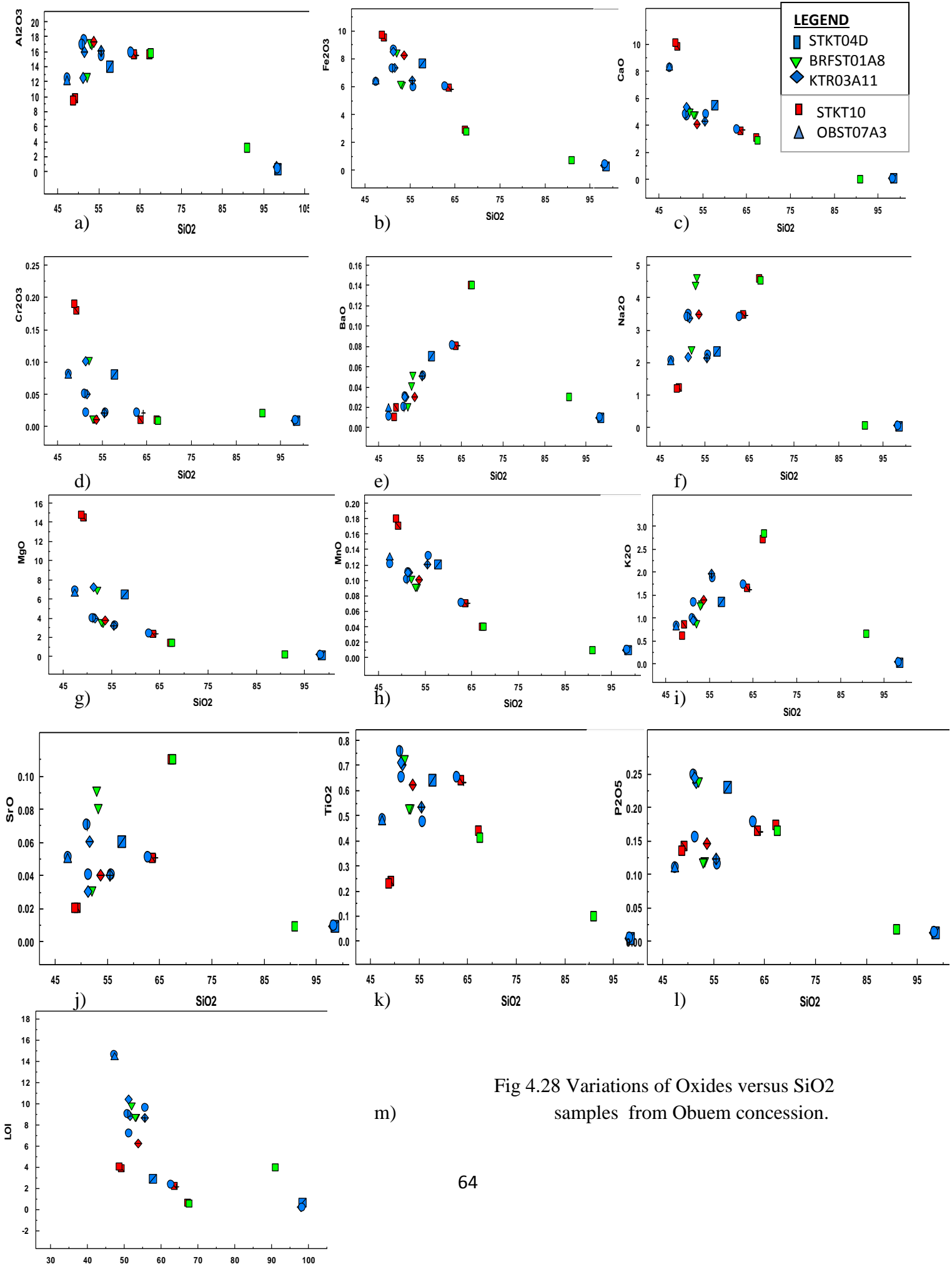


Fig 4.28 Variations of Oxides versus SiO_2 samples from Obuem concession.

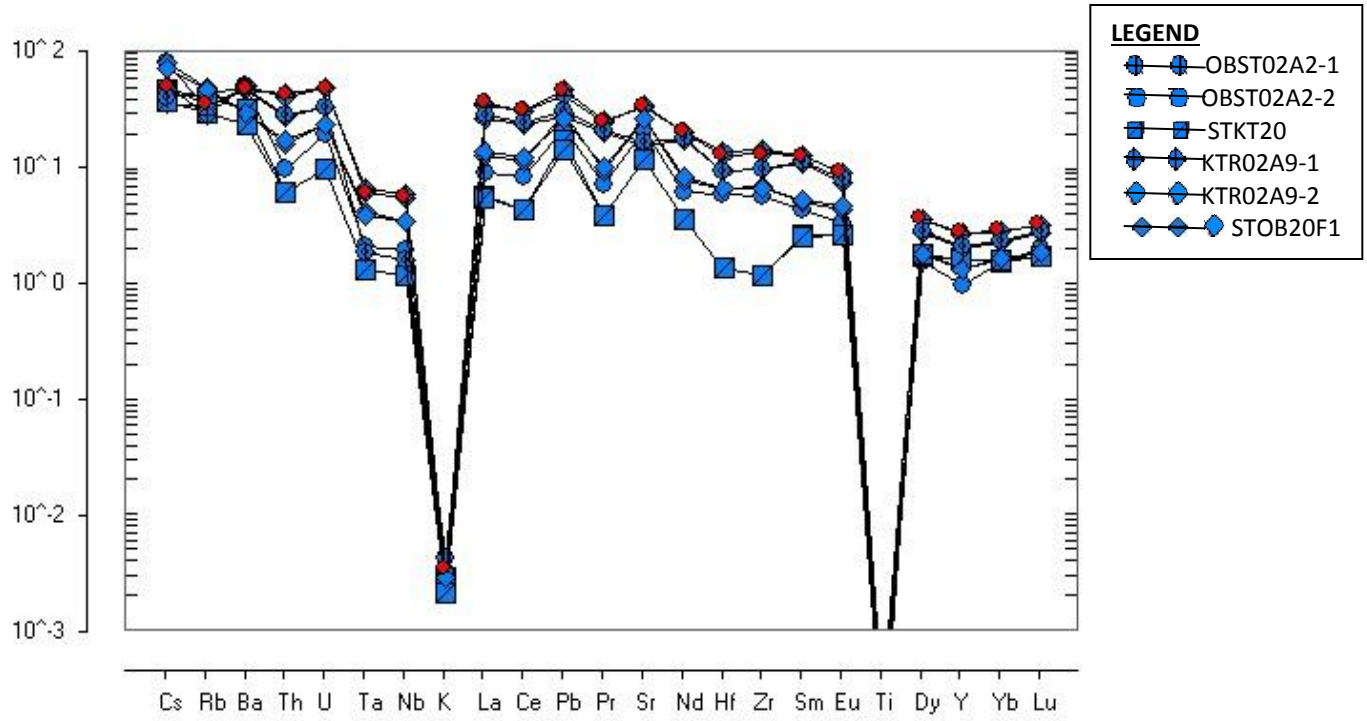


Fig 4.29 Primordial mantle of metavolcanics

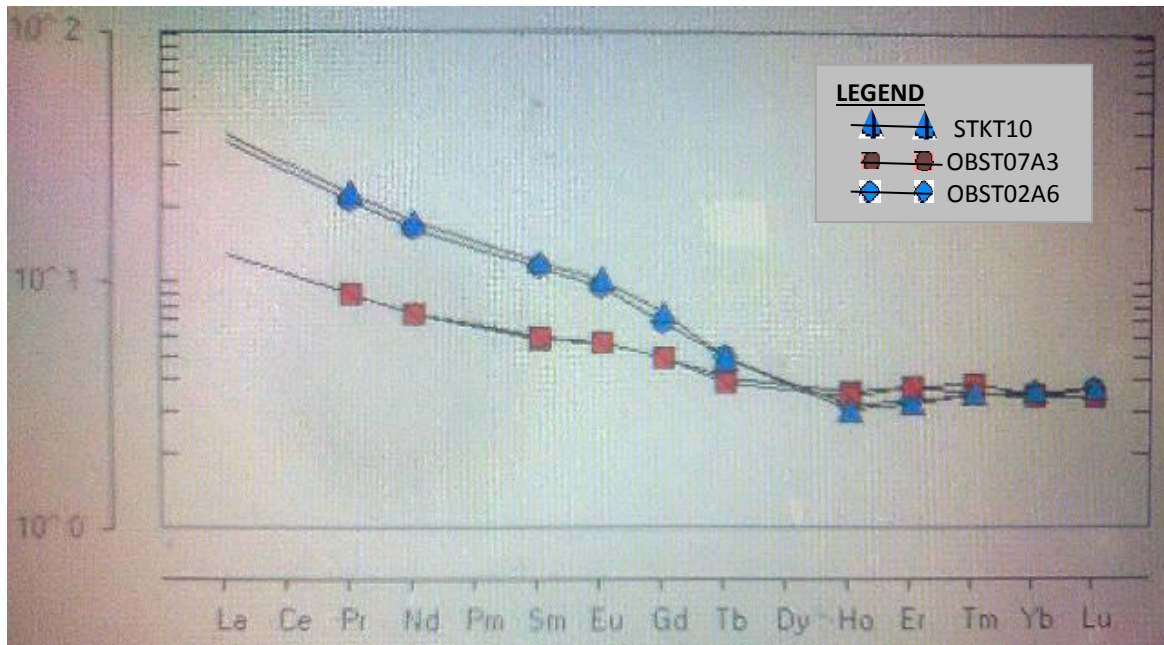


Fig. 4.30 Spider plots for the REE normalized against the Chondrite after Sun & McDonald (1989).

4.3.4. Classification of Granitoids

The granitoids have silica (SiO_2) content of 80 - 90 wt %, alumina (Al_2O_3) values increase from 11 weight percent to 12.40% and that of CaO content ranges from 0.02- 0.03 wt%. The total iron $\text{Fe}_2\text{O}_3 + \text{MgO}$ values range from 0.8 to 0.9wt% whilst alkali ($\text{Na}_2\text{O} + \text{K}_2\text{O}$) values ranged from 0.7-0.8 wt %.

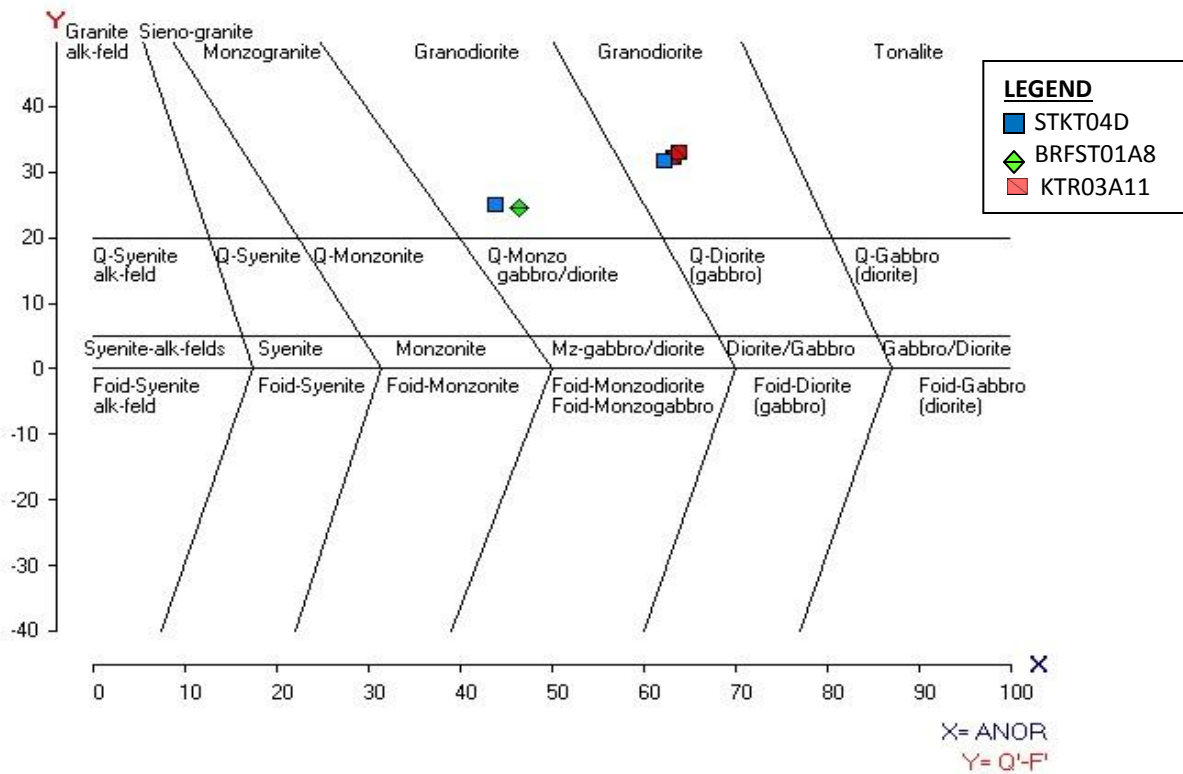


Fig.4.31 The chemical classification of plutonic rocks using their molecular normative compositions diagram. (after Streckeisen and Le Maitre 1979)

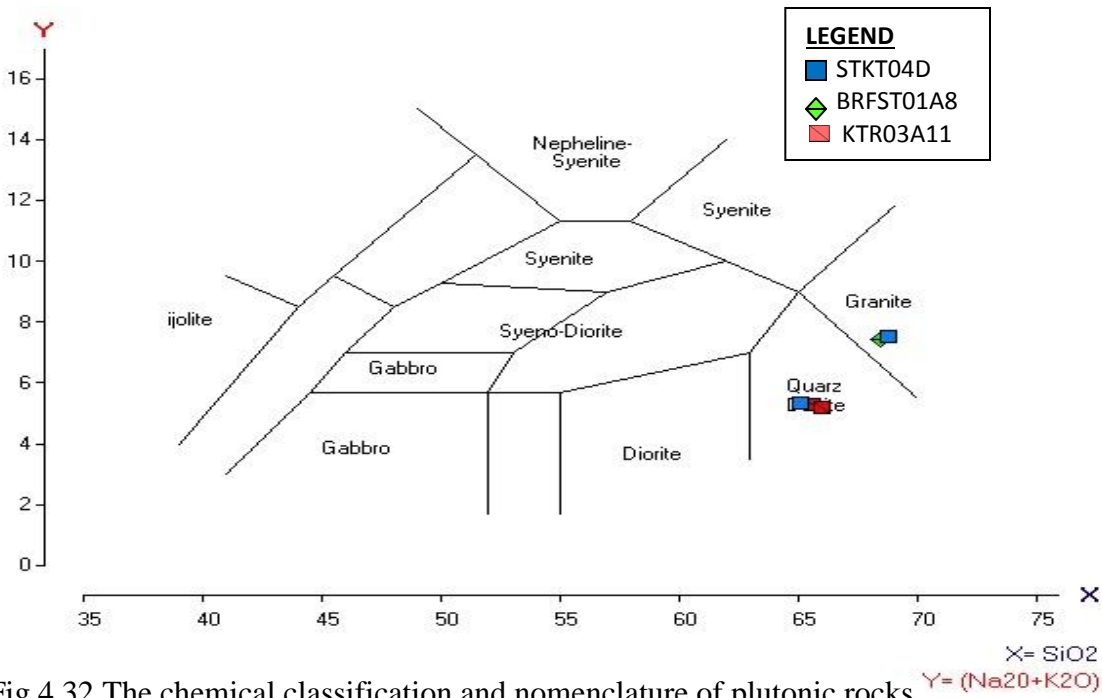


Fig 4.32 The chemical classification and nomenclature of plutonic rocks using the total alkalis versus silica (TAS) diagram. (after Cox et al, 1979)

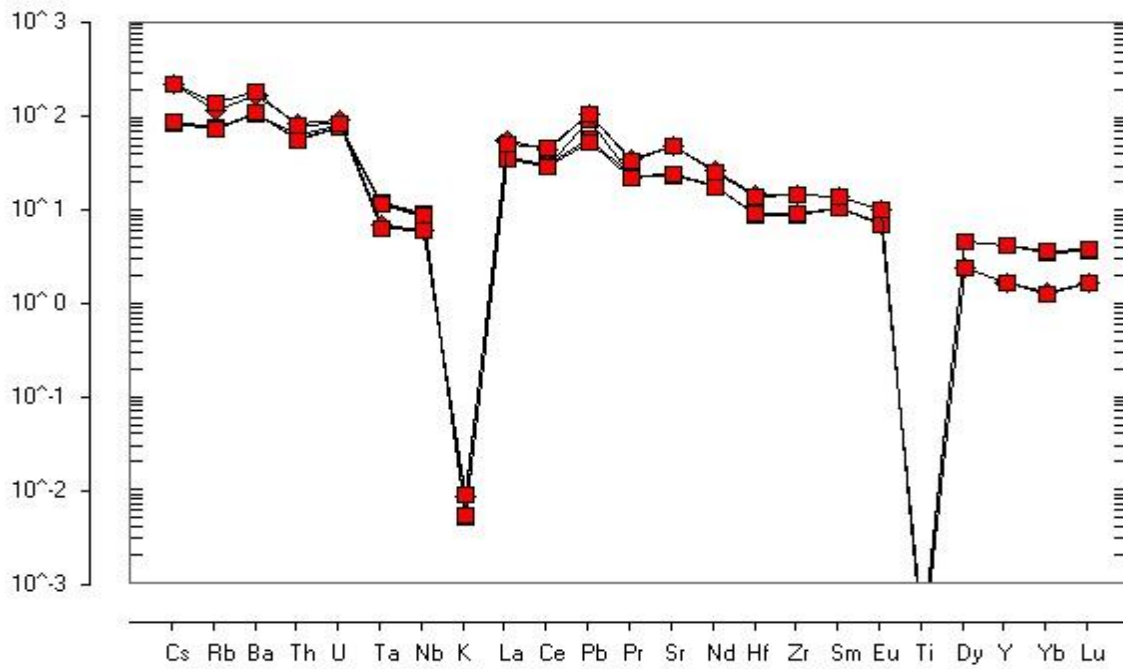


Fig 4.33 Primordial mantle of granitoids

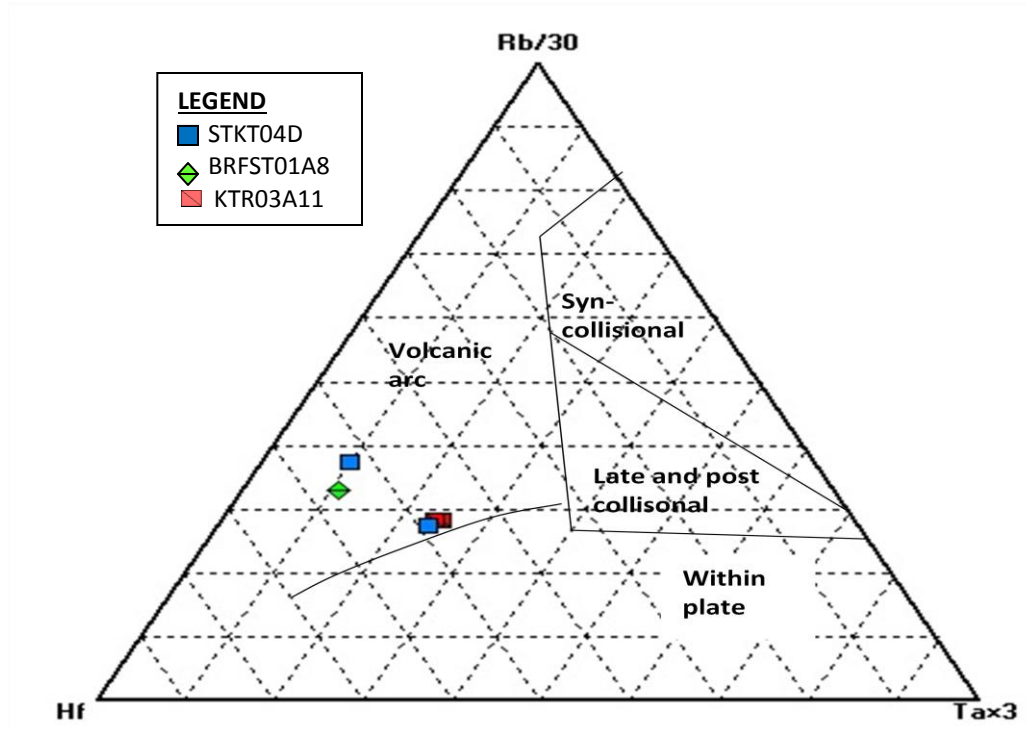


Fig 4.34 Hf-Rb/30-Ta×3 discriminant diagram of arc maturity for volcanic granitoids (after Harris et al, 1986)

CHAPTER FIVE

5.0 DISCUSSION

5.1 MAGMA SOURCE AND TECTONIC SETTINGS

Where it is exposed, at one locality in the west flank of the belt near Kongo (Fig. 5.2), fine-grained sediments are in contact with a foliated, coarse-grained hornblende granodiorite, and the sediment is metasomatized to a hornblende schist and injected with granodiorite material; angular blocks of metasediments are enclosed in the granodiorite and clearly indicate an intrusive relationship between granodiorite and sediments at this contact.

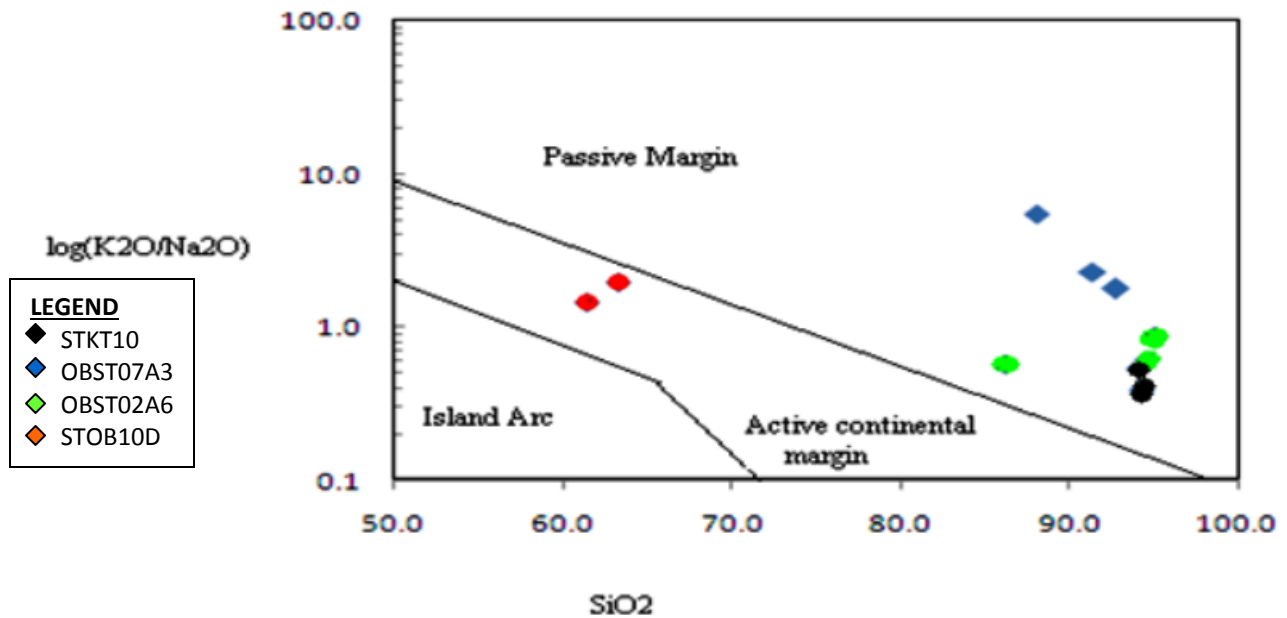


Fig 5.1 Plot showing the tectonic settings of the metasediments

5.1.1 Tectonic settings.

Eoeburnean deformation event (D1) that produced significant deformation in the Birimian metavolcanics b), is associated with N-S shortening manifested as regional scale folding in the Ashanti Belt (Allibone et al., 2002a) . A North – South striking foliation occurs in the schists and Graphitic phyllites on the east flank between Obuem and Kokotro and is discontinuous with the ENE cleavage of the mafic volcanic belt. Farther west from the contact, towards Dotom, the foliation in the Phyllites strikes from N to NE. Thus, in the study area there is only limited evidence for pre-Birimian (basement) granitic rocks and this is inferred from the observation that the NS foliation in the Chlorite Schist, Mica Schist, and Graphitic phyllites and lightly oblique to the NE to ENE striking foliation in the volcanic and sedimentary rocks.

Abundant granites and granitoids intruded the Birimian and Tarkwaian units during the Paleoproterozoic. In Ivory Coast, on the basis of recent mapping and geochronology, Papon (1973) has identified Archaean granitic rocks which are considered to be basement to the Birimian but In contrast, granitoids are unfoliated and were dated at 2171 ± 2 Ma (Hirdes et al., 1992) and 2159 ± 2 Ma (Attoh et al., 2006).

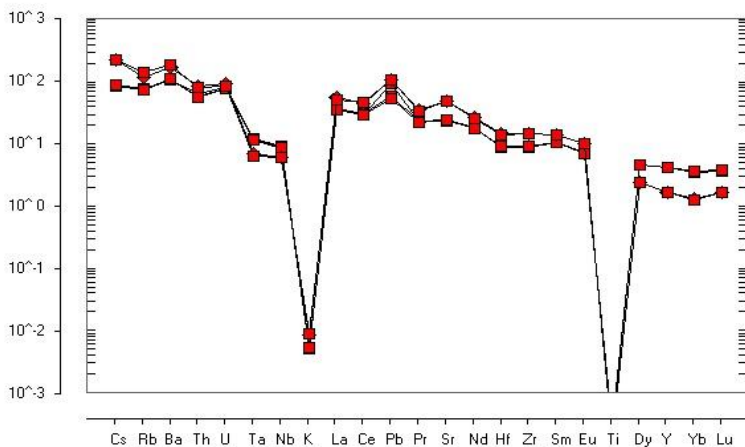


Fig 5.2a Primordial mantle of granitoids

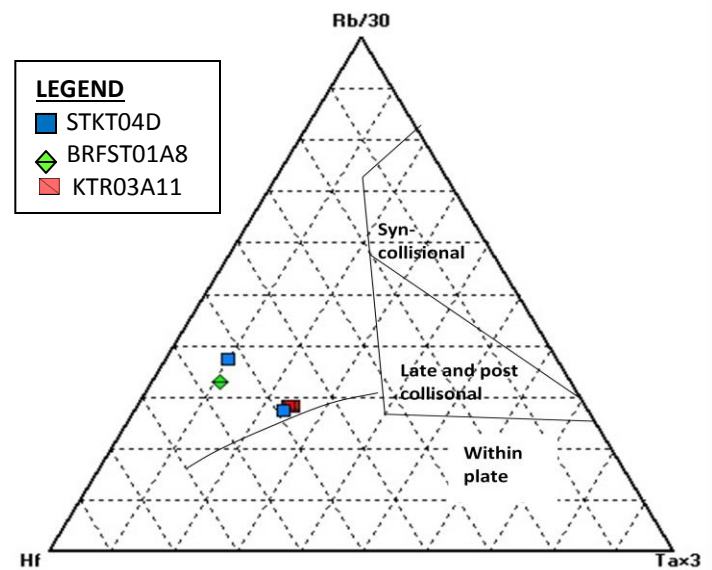


Fig 5.2b Hf-Rb/30-Ta \times 3 discriminant diagram of arc maturity for volcanic granitoids (after Harris et al, 1986)

5.2 TECTONIC EVOLUTION AND DEFORMATION

The sequence of structural event has become clear from the time of volcanism which seems to have occurred at about 2.2 Ga (Perrouy., et al 2002). The area has undergone regional (dynamothermal metamorphism) and dynamic metamorphism. Regional metamorphism alters rocks of thousands of square kilometers in an areas and this resulted in the metamorphic rocks such as quartzites and schist. The dynamic metamorphism results in deformational structures such as foliations and joints. This dynamic metamorphism results in shear zones which produced the schistosity of the metasediments (Chernicoff, 1999).

Eoeburnean deformation event D1 is associated with N-S shortening manifested as regional scale folding in the southern Ashanti Belt (Allibone et al., 2002a). Syn-D1 gold mineralisation associated with quartz veining could be the original source of Tarkwaian paleo-placers and/or remobilised gold concentrations along major shear zones. The presence of quartz veins in the rocks also affirms the dynamic nature of the metamorphism.

The quartz veins are thus sure indication that the area has experienced some level of tectonic activity and also indicate that there has been a minute amount metamorphism occurring. The veins underwent ductile and brittle post-crystallization deformation and are usually seen on foliation surfaces and result from host rocks due to deformational stresses and consequently mobilization and recrystallization of quartz to fill the already existing fractures (Raymond, 1995).

Feybesse et al., (2006) also proposed a significant period of rifting between 2148 – 2125 Mas.

The area lies within the greenschist facies, Ahmed et al (1977).

Observed folding may have developed during the shearing from the Eburnean orogeny, and it is associated with most of the hydrothermal gold deposits in this region.

The outcrop is jointed, with closely spaced nature of the joints suggesting high level of deformational activity. The graphite phyllites show such strong deformation especially at the contact to the metavolcanics. The rock has been moderately deformed and some grains have been welded into their neighbours or penetrating them slightly. Alignment of micaceous minerals in a particular orientation may probably be as a result of small degree of deformation.

5.3 MINERALISATION

Ashanti belt of Ghana which is the key district of gold mineralization in the Paleoproterozoic terrane of West Africa and consists of lithologies of the volcanic-sedimentary Birimian Super group. Konyaw – Obuem Gold which lies on the North-Eastern flank of this same belt is of no exception as mineralisation of gold is closely associated with the sulphides in both quartz veins and alteration zones and this is normally observed within the metavolcanic and metasediments. Petrographic and thin section analyses on the veins of quartz trace them to the primary sin D1 of Allibone et al. (2002a).

Regional foliation and sub parallel shear zones hosting mesothermal gold mineralization developed during deformation coeval with metamorphism. Three major types of primary gold mineralization are present in the Ashanti belt:

- (1) Mesothermal, generally steeply dipping quartz veins in shear zones mainly in Birimian sedimentary rocks (Tunks et al., 2004a)
- (2) Sulfide ores with auriferous arsenopyrite and pyrite, spatially closely associated with the quartz veins (Blenkinsop et a., 1994), and
- (3) Sulfide disseminations and stockworks in granitoids (Luebe et al., 1990).

The first two types of mineralisation in the Birimian are hosted by metavolcanics and metasedimentary units as such as the basaltic andesites, metagreywackes, phyllites, and schists. Intensive studies were not than on the sulphides but can be inferred from thin section and microstructural analysis that there is more than one phase of pyritisation present.

Oberthür et al. (1994) indicated that mineralisation was emplaced during all stages of deformation. Also Luebe et al., (1990), delineated that disseminated sulphides that occur in variety of rock types have been identified as a source of large tonnages of low grade ore in the Birimian. Syn-D1 gold mineralisation associated with quartz veining could be the original source of remobilised gold concentrations along the major shear zones within this concession.

5.4 METAMORPHISM AND ALTERATION

The wavy extinction, stretched or crystal elongation, sutured boundaries, and intragranular cracks of the crystals supports the mechanical aspect of the metamorphism while preferred orientation of linear fabrics, foliation and the fabric of platy minerals in the area are characteristic features of regional metamorphism. The secondary quartz was crystallized after the activities of metamorphism and is therefore interstitial to the primary ones that are not strained. This indicates the severity of metamorphic condition of the area.

Veins form when fluids penetrate a fracture and precipitate minerals. The presence of veins in metamorphic rock suggest that fluids were present (Nishiyama, 1989;, Yardley, 1983).

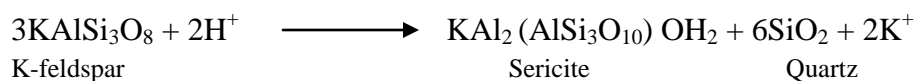
From the mineralogical assemblage and structures in the rock, the metamorphism of the area can be deduced. The rocks making up the metavolcanics and the metasediments in the area namely;

the basaltic andesites, phyllites, metagreywackes, schists and the quartzites have undergone low-grade regional metamorphism. The mineralogical assemblage of quartz, muscovite (sericite), iron-oxide, albite of the rock assemblages also depicts the muscovite, chlorite subfacies of the green schist facies, that is, low pressure and low temperature. Quartz which is the dominant mineral in the rocks within area, from mineralogical description is alpha quartz. This quartz is typical of low grade metamorphic environments.

Most of the minerals observed in the metasediments and the metavolcanics are rocks have been minutely altered or are altering (grain shape and composition). There are some sorts of chloritization seen in the hornblende and biotite and sericitization also occur in the feldspars especially the Plagioclase.

In thin sections the quartz grains show deformed edges, some degree of crystallization and some elongation. This implies that some level of metamorphism has occurred but may be minimal. Low grade metamorphism retains enough of their original character such as bedding and other sedimentary structures with original minerals. Low grade metamorphism occurs at relatively low temperature (200°C – 400°C, or 400°F – 750°F) and pressures (about 1-6 kilo bars). The following are the relevant metamorphic processes that took place at the mapped area.

Sericitization is alteration process that involves the alteration of k-feldspar, plagioclase, Al_2SiO_5 polymorphs, cordierite, and staurolite to fine grained aggregates of muscovite (sericite). These are commonly speckled with or completely pseudomorphed. The growth of sericite most notably requires the addition of water and, K-feldspar, and sericitization can only proceed if water-rich fluids are available (Shelley, 1993). Sericitization is expressed in a chemical equation as:



More sericites are formed if the acid content (H^+) increases shifting the equation to the right. Diffusion is the rate - controlling factor in sericitization: for reaction depends on the supply of fluid and K^+ yet the products grow only at the local sites of reaction (e.g. particular zone within plagioclase), presumably due to the relative immobility of Si and Al.

Chloritization on the other hand involves extensive replacement of original assemblage by chlorite influx of aqueous fluids; a retrograde associate with hydrothermal alteration of mafic rocks and green schist facies occurring along shear zones. Chloritization is one of the subdivisions of propylitization. The K^+ released from biotite sericitizes plagioclase and Ca^+ release from the plagioclase is used to produce epidote, and titanite, mixed in which sheet silicates (Shelley, 1993).

The chemical equation is given by (Raymond, 1995) as:



CHAPTER SIX

6.0 CONCLUSION AND RECOMMENDATION

6.1 CONCLUSION

Lithological mapping and sampling of pit rocks were successfully carried out and petrographical analyses which include study of mineralogical composition, textures, structural features and any alteration features were done.

Petrological study of the pit rocks identified meta-sediments, meta-volcanics, granitoids and quartzites as main rock types.

The metasediments seen on the field are mainly metamorphosed phyllites, schist and metagreywackes.

Two forms of phyllites were encountered. These are the evenly foliated brown to grey phyllite and the graphitic phyllites which are black and have silky luster.

For the metamorphosed schist, it has medium to coarse grained texture, the fabric of which is characterized by an excellent parallelism or schistosity.

The greywackes show grey, grained well-indurated and crystalline rock composed of mixed up grains of easily destroyed minerals of rock fragments. Major framework grains are quartz and feldspars, which together with lithic fragments are cemented in a clayey matrix.

The Metavolcanics encountered was calcareous chlorite-schists which has phaneritic texture with hardly visible mineral crystals. Hornblende and biotite make up the mafic crystals and the light

colored crystals comprise the plagioclase feldspar, Quartz and K-feldspar. The presence of chlorite gives the rock its greenish colour.

Granitoids shows granitic crystal aggregates of phaneritic texture with large visible holocrystalline crystals. Hornblende and biotite make up the mafic crystals and the light colored crystals comprise the plagioclase feldspar, Quartz and K-feldspar.

Quartzites are grey to white in colour on freshly opened surfaces. The rock is medium crystalline to coarse grained, hard, highly compact and weathered to some extent. They are hard and glassy and are sometimes difficult to distinguish from vein quartz. This probably resulted from the recrystallization of quartz grains. The minerals present in the rock are mainly quartz are sometimes stained with iron. The rocks are very well indurated and less porous.

Structural mapping revealed two sets of joints are present in the area. These joints have various orientations but tend to follow two major trends at nearly right angles. The joint usually cut across foliation and hence deduced to be younger. Joints in these outcrops have their strike parallel to the general strike of the area. The rocks in the area generally have a NW/SE strike, have two general directions of dip which are opposite with most in a NE and SW direction.

The veins are usually seen on foliation surfaces and result from host rocks due to deformational stresses and consequently mobilization and recrystallization of quartz to fill the already existing fractures. The quartz veins have been squeezed out of the rock formation possibly due to compressive stress of the overlying rocks or differential weathering

The anticline had a trend of 020 NNE and plunge of 80° ENE. This anticline has a width of 3.0 cm. The amplitude of the fold is 2m.

The foliations were observed in both the metavolcanics and the metasediments. The foliations formed as a result of ductile responses to incident stress causing realignment of minerals in the direction of least stress. It can be inferred that the forces that caused the deformation were from NW-SE and NE-SW.

Geochemistry of the Obuem Metavolcanics indicated they are basalt and andesitic-basalt of calc-alkaline nature. The chemical classification and nomenclature of plutonic rocks shows rock to be granodiorite, granite and quartz-diorite,

Alteration patterns of minerals and geochemical analysis as well as their moderate to high chemical index of alteration values suggests that these rocks experienced a relatively weak to moderately high chemical weathering from a basaltic source rock.

Average Cr and Ni abundances and Cr/Ni ratios of average phyllites of the Birimian metasediments indicate that the source consisted of basaltic material.

The transition metal geochemistry as well as $\text{SiO}_2\text{-K}_2\text{O/Na}_2\text{O}$ binary plot also support that these phyllites originated from a mafic igneous source and were deposited in an active continental margin setting.

Studying the deformation and alteration history, conclusion can be made that gold mineralization in the study area is primary hydrothermal gold lodes (quartz+pyrite) emplaced during D1 and the ore geometry is controlled mainly by fold patterns and shear zones.

6.2 RECOMMENDATION

Though a lot has been done with geological mapping in this study area, it would be of good if massive geophysical data are obtained. Furthermore, more intense structural mapping or studies should be carried out by researchers or fellow Geologist.

REFERENCES

- Adadey, K., Clarke, B., Théveniaut, H., Urien, P., Delor, C., Roig, J.Y., Feybesse, J.L., 2009. Geological map explanation—Map sheet 0503 B (1:100 000), CGS/BRGM/Geoman. Geological Survey Department of Ghana (GSD). No MSSP/2005/GSD/5a.
- Affaton, P., Rahman, M.A., Trompette, R., and Sougy, J., 1991. The Dahomeyide orogeny: Tectonothermal evolution and relationship to Volta basin, In Dallmeyer, R.D., and Lecorche, J-P., (eds.), *The West Africa Orogens and Circum- Atlantic Correlatives*: New York, Springer-Verlag, pp95-111.
- Ahmed, S.M., Blay, P.K., Caster, S.B., Coakley, G.J., 1977. The geology of ¼ field sheets. Ghana Geological Survey, Bulletin No. 32, pp 16-19, 30 -34.
- Agyei Duodu, J., Loh, G.K., Boamah, K.O., Baba, M., Hirdes, W., Toloczyki, M., Davis, D.W., 2009. Geological map of Ghana 1:1 000 000. Geological Survey Department of Ghana (GSD).
- Akarish, A.I.M., El-Gohary, A.M., (2008). Petrography and Geochemistry of lower Paleozoic Sandstones, East Sinai, Egypt. Implications for Provenance and Tectonic Setting. *African Earth Sciences*, pp 8-18
- Allibone, A., McCuaig, T.C., Harris, D., Etheridge, M., Munroe, S., Byrne, D., 2002a. Structural controls on gold mineralization at the Ashanti Gold Deposit, Obuasi, Ghana. *Society of Economic Geologists (Special Publication) 9*, 65–93.
- Allibone, A., Teasdale, J., Cameron, G., Etheridge, M., Uttley, P., Soboh, A., Appiah-Kubi, J., Adanu, A., Arthur, R., Mamphey, J., Odoom, B., Zuta, J., Tsikata, A., Pataye,

F., Famiyeh, S., Lamb, E., 2002b. Timing and structural controls on gold mineralization at the Bogoso Gold Mine, Ghana, West Africa. *Economic Geology* 97, 949–969.

Asiedu, D. K., Banoeng-Yakubo, B., Manu, J. and Nyarko, B.J.B, (2004). Geochemistry of Paleozoic metasedimentary rocks from the Birim diamondiferous fields, southern Ghana: Implications for Provenance and crustal evolution at the Archean-Proterozoic boundary. *Geochemical Journal*, vol. 38, pp. 215 to 228.

Attoh, K., 1990. Dahomeyides of southeastern Ghana: Evidence for oceanic closure and crustal imbrications in a Pan African orogeny. 15th coll. *African Geol.* pp150-164.

Attoh, K., Dallmeyer, R.D., and Affaton P., 1997. Chronological nappe assemblage in the Pan African Dahomeyide orogeny, West Africa. Evidence from $^{40}\text{Ar}/^{39}\text{Ar}$ mineral ages. *Precambrian research*, pp 82, 135-137.

Attoh, K., Evans, M.J., Bickford, M.E., 2006. Geochemistry of an ultramafic-rodingite rock association in the Paleoproterozoic Dixcove greenstone belt, southwestern Ghana. *Journal of African Earth Sciences* 45, 333–346.

Baratoux, L., Metelka, V., Naba, S., Jessell, W.M., Gregoire, M., Ganne, J., 2011. Juvenile Paleoproterozoic crust evolution during the Eburnean orogeny (–2.2-2.0 Ga), Western Burkina Faso. *Precambrian Research* 191, 18–45.

Barritt, S.D., Kuma, J.S., 1998. Constrained gravity models and structural evolution of the Ashanti Belt, southwest Ghana. *Journal of African Earth Sciences* 26 (4), 539–550.

Benneh, M.P., Dickson, K.B., 1990, A New geography of Ghana. pp 20-32, 36-38

Bhatia, M.R., 1983. Plate tectonics and geochemical composition of sandstones .J. Geol, 91,611-627

Blenkinsop, T.G., Schmidt Mumm, A., Kumi, R., Sangmor, S., 1994. Structural geology of the Ashanti Gold Mine. Geologisches Jahrbuch D 100, 131–153.

Bonhomme, M., 1962. Contribution à l'étude géochronologique de la plate-forme de l'Ouest African. Ann. Fac. Sci. Univ. Clermont-Ferrand Géol. Minéral. 5, 62.

Bowell, R.J., Foster, R.P., Stanley, C.J., 1990. Telluride mineralization at Ashanti gold mine, Ghana. Mineralogical Magazine 54, 617–627.

Chaloner, W.G., Mensah, M.K., Crane, M.D., 1974. Non-vascular land plants from the Devonian of Ghana. Paleontology 17 (4), 925–947.

Clark, D.A., 1997. Magnetic petrophysics and magnetic petrology: aids to geological interpretation of magnetic surveys. AGSO Journal of Australian Geology and Geophysics 17 (2), 83–103.

Compton R.R., 1962. Manual in field geology, John Wiley and Sons, New York.

De Sitter, L.U., 1956. Structural geology, McGraw-Hill book company, Inc., pp 87-88, 93-98

Crow, A.T., 1952. The rocks of the Sekondi Series of the Gold Coast. Gold Coast Geological Survey 18, 68.

Dampare, S.B., Shibata, T., Asiedu, D.K., Osaе, S., Banoeng-Yakubo, B., 2008. Geochemistry of Paleoproterozoic metavolcanic rocks from the southern Ashanti volcanic belt, Ghana: petrogenetic and tectonic setting implications. Precambrian Research 162, 403–423.

Davis, D.W., Hirdes, W., Schaltegger, U., Nunoo, E.A., 1994. U–Pb age constraints on

deposition and provenance of Birimian and gold-bearing Tarkwaian sediments in Ghana, West Africa. *Precambrian Research* 67, 89–107.

De Kock, G.S., Armstrong, R.A., Siegfried, H.P., Thomas, E., 2011. Geochronology of the Birim Supergroup of the West African craton in the Wa-Bolé region of westcentral Ghana: implications for the stratigraphic framework. *Journal of African Earth Sciences* 59, 1–40.

Dickson, B.L., Scott, K.M., 1997. Interpretation of aerial gamma-ray surveys—adding the geochemical factors. *AGSO Journal of Australian Geology and Geophysics* 17 (2), 187–200.

Eisenlohr, B.N., 1992. Conflicting evidence on the timing of mesothermal and paleoplacer gold mineralisation in early Proterozoic rocks from southwest Ghana, West Africa. *Mineralium Deposita* 27, 23–29.

Eisenlohr, B.N., Hirdes, W., 1992. The structural development of the early Proterozoic Birimian and Tarkwaian rocks of southwest Ghana, West Africa. *Journal of African Earth Sciences* 14 (3), 313–325.

Eriksson, K.A., Krapez, B., Fralick, P.W., 1994. Sedimentology of Archean greenstone belts; signatures of tectonic evolution. *Earth-Science Reviews* 37, 1–88.

Feybesse, J.L., Billa, M., Guerrot, C., Duguey, E., Lescuyer, J.L., Milési, J.P., Bouchot V., 2006. The paleoproterozoic Ghanaian province: geodynamic model and ore controls, including regional stress modeling. *Precambrian Research* 149, 149–196.

Griffis, R.J., Barning, K., Agezo, F.L., Akosah, F.K., 2002. Gold Deposits of Ghana. Minerals Commission, Accra, Ghana, p. 438.

Gunn, P.J., Maidment, D., Milligan, P.R., 1997. Interpreting aeromagnetic data in areas of limited outcrop. *AGSO Journal of Australian Geology and Geophysics* 17 (2), 175–185.

Hastings, D.A., 1982. On the tectonics and metallogensis of West Africa, A model incorporating new geophysical data. *Geoexploration* 20, 295–327.

Hein, K.A.A., 2010. Succession of structural events in the Goren greenstone belt (Burkina Faso): implications for West African tectonics. *Journal of African Earth Sciences* 86, 77–89.

Hirdes, W., Davis, D.W., 1998. First U–Pb zircon age of extrusive volcanism in the Birimian Supergroup of Ghana/West Africa. *Journal of African Earth Sciences* 27 (2), 291–294.

Hirdes, W., Davis, D.W., Eisenlohr, B.N., 1992. Reassessment of proterozoic granitoid ages in Ghana on the basis of U/Pb zircon and monazite dating. *Precambrian Research* 56, 89–96.

Hirdes, W., Nunoo, B., 1994. The proterozoic paleoplacers at Tarkwa Gold Mine, SW Ghana: Sedimentology, mineralogy, and precise age dating of the main reef and west reef, and bearing of the investigations on source area aspects. *Geologisches Jahrbuch D* 100, 247–311.

Hünken, U., Klemd, R., Olesch, M., 1994. Fluid inclusions in quartz-pebbles of proterozoic tarkwaian conglomerates in Ghana. *Geologisches Jahrbuch D* 100, 313–341.

Jessell, M.W., 1981. Noddy—an interactive map creation package. M.Sc. Thesis, University of London, England, 49 p.

Jessell, M.W., Valenta, R.K., 1996. Structural geophysics: integrated structural and geophysical mapping. In: DePaor, D. (Ed.), *Structural Geology and Personal Computers*. Elsevier, Oxford, pp. 303–324.

Jessell, M.W., 2001. Three-dimensional geological modelling of potential-field data. *Computers and Geosciences* 27, 147–157.

John, T., Klemd, R., Hirdes, W., Loh, G., 1999. The metamorphic evolution of the Paleoproterozoic (Birimian) volcanic Ashanti belt (Ghana, West Africa). *Precambrian Research* 98, 11–30.

Junner, N.R., 1932, The geology of the Obuasi goldfield. Memoir of the Gold Coast Geological Survey 2: 43 p. —1935, Gold in the Gold Coast. Memoir of the Gold Coast Geological Survey, v. 4: 67 p.

Junner, N.R., 1935. Gold in the Gold Coast. Gold Coast Geological Survey, Memoir No. 4, 76 p.

Kesse, G.O., 1985, The mineral resources of Ghana, A.A. Belkema Publishers, The Netherlands-Rotterdam.

Le Bas, M.J., Le Maitre, R.W., Streckeisen, A., Zanettin, B., 1986. A chemical classification of volcanic rocks based on the total alkali-silica diagram. *Journal of Petrology* 27, 745-750.

Mani, R., 1978, The geology of the Dahomeyan of Ghana. Geology of Ghana project. Geological survey (Unpublished report).

Manu, J., Asiedu, D. K., and Anani, C. Y., 2003. Geochemistry of Birimian phyllites from the Obuasi and Prestea Mines, Southwestern Ghana: Implications for provenance and source-area weathering. *International Journal of Basic and Applied Sciences*, 2 (1) pp 12-19

McLennan, S. M., Hemming, S. R., Taylor, S. R., and Eriksson, K.A., (1995). Early Proterozoic Crustal Evolution: Geochemical and Nd-Pb isotopic evidence from metasedimentary rocks, southern America. *Geochem. Acta* 59, 1153-1177.

Milesi, J.P., Ledru, P., Ankrah, P., Johan, V., Marcoux, E., Vinchon, Ch., 1991. The metallogenic relationship between Birimian and Tarkwaian gold deposits in Ghana. *Mineralium Deposita* 26, pp 228–238.

Milési, J.P., Ledru, P., Feybesse, J.L., Dommanget, A., Marcoux, E., 1992. Early Proterozoic ore deposits and tectonics of the Birimian orogenic belt, West Africa. *Precambrian Research* 58, pp 305–344.

Milesi, J. P., Feybesse, J. L., Ledru, P., et al., “ Les mineralisations auriferes de l’Afrique de l’Ouest. Leur evolution lithostructurale au Proterozoique inferieur, Carte metallogenique a 1/2 000 000”, *Chronique de la recherche miniere, France*, Vol. 497, (1989), pp. 98

Raymond, L.A., 1995, *Petrology*, McGraw-Hill publishers, pp 476-479.

Milligan, P.R., Gunn, P.J., 1997. Enhancement and presentation of airborne geophysical data. *AGSO Journal of Australian Geology and Geophysics* 17 (2), 63–75.

Mumin, A.H., Fleet, M.E., 1995. Evolution of gold mineralization in the Ashanti Gold Belt, Ghana: evidence from carbonate compositions and parageneses. *Mineralogy and Petrology* 55, pp 265–280.

Mumin, A.H., Fleet, M.E., Chryssoulis, S.L., 1994. Gold mineralization in As-rich mesothermal gold ores of the Bogosu-Prestea mining district of the Ashanti Gold Belt, Ghana: remobilization of invisible gold. *Mineralium Deposita* 29, 445–460.

Mumin, A.H., Fleet, M.E., Longstaffe, F.J., 1996. Evolution of hydrothermal fluids in the Ashanti Gold Belt, Ghana: stable isotope geochemistry of carbonates, graphite, and quartz. *Economic Geology* 91, 135–148.

Ntiamoah-Agyakwa, Y., 1979. Relationship between gold and manganese mineralizations in the Birimian of Ghana, West Africa. *Geological Magazine* 116, 345–352.

Nyame, F.K., Kase, K., Yamamoto, M., 1998. Spessartine garnets in a manganiferous carbonate formation from Nsuta, Ghana. *Resource Geology* 48 (1), 13–22.

Oberthür, T., Vetter, U., Davis, D.W., Amanor, J.A., 1998. Age constraints on gold mineralization and Paleoproterozoic crustal evolution in the Ashanti belt of southern Ghana. *Precambrian Research* 89, 129–143.

Oberthür, T., Vetter, U., Schmidt Mumm, A., Weiser, T., Amanor, J.A., Gyapong, W.A., Kumi, R., Blenkinsop, T.G., 1994. The Ashanti Gold Mine at Obuasi, Ghana: Mineralogical, geochemical, stable isotope and fluid inclusion studies on the metallogenesis of the deposit. *Geologisches Jahrbuch D* 100, 31–129.

Oberthür, T., Weiser, T., Amanor, J.A., Chryssoulis, S.L., 1997. Mineralogical siting and distribution of gold in quartz veins and sulfide ores of the Ashanti mine and other deposits in the Ashanti belt of Ghana: genetic implications. *Mineralium Deposita* 32, 2–15.

Pearce, J.A., Cann, J.R., 1973. Tectonic setting of basic volcanic rocks determined using trace element analyses. *Earth and Planetary Science Letters* 19, 290-300.

Pigois, J.P., Groves, D.I., Fletcher, I.R., McNaughton, N.J., Snee, L.W., 2003. Age constraints on Tarkwaian palaeoplacer and lode-gold formation in the Tarkwa- Damang district, SW Ghana. *Mineralium Deposita* 38, 695–714.

Middlemost, E.A.K., 1975. The basalt clan. *Earth Sciences Review* 11, 337-364.

Schmidt Mumm, A., Oberthür, T., Vetter, U., Blenkinsop, T.G., 1997. High CO₂ content of fluid inclusions in gold mineralisations in the Ashanti Belt, Ghana: a new category of ore forming fluids? *Mineralium Deposita* 32, 107–118.

Roser, B.P., Korsch, R.J., “Determination of tectonic setting of sandstone- mudstone suites using SiO₂ content and K₂O/Na₂O ratio”, *Journal of Geology*, Vol. 94, (1986), pp. 635-650.

Roser, B.P., Korsch, R.J., 1988. Provenance signatures of sandstone-mudstone suites determination using discriminate function analysis of major element data. *chem.Geol.* 67, 119-139

Schwartz, M.O., Oberthür, T., Amanor, J., Gyapong, W. A., 1992. Fluid inclusion re-equilibration and P-T-X constraints on fluid evolution in the Ashanti gold deposit, Ghana. *European Journal of Mineralogy* 4, 1017–1033.

- Sestini, G., 1973. Sedimentology of a Paleoplacer: the gold-bearing Tarkwaian of Ghana. Ores in Sediments, International Union of Geological Sciences, Series A 3, 275–305.
- Sun, S.S., McDonough, W.F., 1989 Chemical and isotopic systematics of ocean basalts: implications for mantle composition and processes. In: Saunders A.D. and Norry M.J. (eds), Magmatism in ocean basin. Geol. Soc. London. Spec. Pub. 42, 313-345.
- Taylor, P.N., Moorbath, S., Leube, A., Hirdes, W., 1992. Early Proterozoic crustal evolution in the Birimian of Ghana: constraints from geochronology and isotope geochemistry. Precambrian Research 56, 97–111.
- Tevendale, W.B., 1950. Annual report 1948–49. Gold Coast Geological Survey, 32.
- Tshibubudze, A., Hein, K.A.A., Marquis, P., 2009. The Markoye shear zone in NE Burkina Faso. Journal of African Earth Sciences 55, 245–256.
- Tunks, A.J., Selley, D., Rogers, J.R., Brabham, G., 2004. Vein mineralization at the Damang Gold Mine, Ghana: controls on mineralization. Journal of Structural Geology 26, 1257–1273.
- Talwani, M., Heirtzler, J.R., 1964. In: Parks, G.A. (Ed.), Computation of Magnetic Anomalies Caused by Two-Dimensional Bodies of Arbitrary Shape. Computers in the Mineral Industries. School of Earth Sciences, Stanford University, pp 464–480.
- Talwani, M., Worzel, J.I., Landisman, M., 1959. Rapid gravity computations for twodimensional bodies with application to the Mendicino submarine fracture zone. Journal of Geophysical Research 64, 49–59.
- Verduzco, B., Fairhead, J.D., Green, C.M., 2004. New insights into magnetic derivatives for structural mapping. The Leading Edge 29 (1), 24–29.
- Whitelaw, O.A.L., 1929. The Geological and Mining Features of the Tarkwa-Abosso Goldfield. Gold Coast Geological Survey, Memoir No. 1, 46 p.

Wille, S.E., Klemd, R., 2004. Fluid inclusion studies of the Abawso gold prospect, near the Ashanti Belt, Ghana. *Mineralium Deposita* 39, 31–45.

Winkler, G.F., 1974. *Petrogenesis of Metamorphic Rocks*, 3rd ed, Springer-Verlag, New York. Pp 312 – 316.

Yao, Y., Murphy, P.J., Robb, L.J., 2001. Fluid characteristics of Granitoid-Hosted gold deposits in the Birimian Terrane of Ghana: a fluid inclusion microthermometric and Raman spectroscopic study. *Economic Geology* 96, 1611–1643.

Yao, Y., Robb, L.J., 2000. Gold mineralization in Palaeoproterozoic granitoids at Obuasi, Ashanti region, Ghana: ore geology, geochemistry and fluid characteristics. *South African Journal of Geology* 103, 255–278.